

# Transcriptional Regulation of Oncogenic Protein Kinase C $\epsilon$ (PKC $\epsilon$ ) by STAT1 and Sp1 Proteins\*

Received for publication, January 10, 2014, and in revised form, May 5, 2014. Published, JBC Papers in Press, May 13, 2014, DOI 10.1074/jbc.M114.548446

HongBin Wang<sup>‡</sup>, Alvaro Gutierrez-Uzquiza<sup>‡</sup>, Rachana Garg<sup>‡</sup>, Laura Barrio-Real<sup>‡</sup>, Mahlet B. Abera<sup>‡</sup>, Cynthia Lopez-Haber<sup>‡</sup>, Cinthia Rosembli<sup>‡</sup>, Huaisheng Lu<sup>‡</sup>, Martin Abba<sup>§</sup>, and Marcelo G. Kazanietz<sup>‡1</sup>

From the <sup>‡</sup>Department of Pharmacology, Perelman School of Medicine, University of Pennsylvania, Philadelphia, Pennsylvania 19104 and the <sup>§</sup>Centro de Investigaciones Inmunológicas Básicas y Aplicadas, Universidad Nacional de La Plata, CP1900 La Plata, Argentina

**Background:** PKC $\epsilon$ , a kinase widely implicated in tumorigenesis and metastasis, is overexpressed in many cancers.

**Results:** Transcription factors Sp1 and STAT1 control the expression of PKC $\epsilon$  in cancer cells.

**Conclusion:** Up-regulation of PKC $\epsilon$  is mediated by dysregulated transcriptional mechanisms.

**Significance:** Our results may have significant implications for the development of approaches to target PKC $\epsilon$  and its effectors in cancer therapeutics.

Overexpression of PKC $\epsilon$ , a kinase associated with tumor aggressiveness and widely implicated in malignant transformation and metastasis, is a hallmark of multiple cancers, including mammary, prostate, and lung cancer. To characterize the mechanisms that control PKC $\epsilon$  expression and its up-regulation in cancer, we cloned an ~1.6-kb promoter segment of the human PKC $\epsilon$  gene (*PRKCE*) that displays elevated transcriptional activity in cancer cells. A comprehensive deletion analysis established two regions rich in Sp1 and STAT1 sites located between –777 and –105 bp (region A) and –921 and –796 bp (region B), respectively, as responsible for the high transcriptional activity observed in cancer cells. A more detailed mutagenesis analysis followed by EMSA and ChIP identified Sp1 sites in positions –668/–659 and –269/–247 as well as STAT1 sites in positions –880/–869 and –793/–782 as the elements responsible for elevated promoter activity in breast cancer cells relative to normal mammary epithelial cells. RNAi silencing of Sp1 and STAT1 in breast cancer cells reduced PKC $\epsilon$  mRNA and protein expression, as well as *PRKCE* promoter activity. Moreover, a strong correlation was found between PKC $\epsilon$  and phospho-Ser-727 (active) STAT1 levels in breast cancer cells. Our results may have significant implications for the development of approaches to target PKC $\epsilon$  and its effectors in cancer therapeutics.

The serine-threonine kinase protein kinase C $\epsilon$  (PKC $\epsilon$ ), a phorbol ester receptor, has been widely implicated in numerous cellular functions, including cell cycle progression, cytokinesis, cytoskeletal reorganization, ion channel control, and transcription factor activity regulation (1–6). This ubiquitously expressed kinase has been associated with multiple disease conditions, including obesity, diabetes, heart failure, neu-

rological diseases, and cancer (7–10). PKC $\epsilon$  is primarily activated by the lipid second messenger diacylglycerol (11), a product of phosphatidylinositol 4,5-bisphosphate hydrolysis by phospholipase C, which, like phorbol esters, binds to the C1 domains located in the N-terminal regulatory region. Receptors coupled to diacylglycerol generation, including tyrosine kinase and G-protein-coupled receptors, cause the intracellular mobilization of PKC $\epsilon$  to the plasma membrane and other intracellular compartments, where it associates with interacting partners and phosphorylates specific substrates (12).

It is widely recognized that distinct members of the diacylglycerol/phorbol ester-regulated PKCs act either as promoters or suppressors of growth and tumorigenesis (13, 14). In that regard, work from several laboratories identified PKC $\epsilon$  as an oncogenic kinase and established important roles for this kinase in the development and progression of cancer. Early studies revealed that ectopic overexpression of PKC $\epsilon$  leads to malignant transformation in some cell types (11, 15, 16). PKC $\epsilon$  confers growth advantage and survival through the activation of Ras/Raf/ERK, PI3K/Akt, STAT3, and NF- $\kappa$ B pathways (17, 18). PKC $\epsilon$  also mediates resistance to chemotherapeutic agents and ionizing radiation, and inhibition of its activity or expression sensitizes cancer cells to cell death-inducing agents (19–21). Most remarkably, PKC $\epsilon$  emerged as a cancer biomarker, as it is markedly up-regulated in most epithelial cancers (22, 23). For example, the vast majority of prostate tumors, in particular those from advanced and recurrent patients, display elevated PKC $\epsilon$  levels (24). Prostate-specific PKC $\epsilon$  transgenic mice develop prostatic neoplastic lesions with elevated Akt, STAT3, and NF- $\kappa$ B activity (17). Another remarkable example of PKC $\epsilon$  up-regulation is in lung cancer; the vast majority (>90%) of primary human non-small cell lung cancers show significant PKC $\epsilon$  overexpression compared with normal lung epithelium, and knockdown of PKC $\epsilon$  from non-small cell lung cancer cells impairs their ability to form tumors and metastasize in nude mice (25). Likewise, depletion of PKC $\epsilon$  from breast cancer cells impairs growth, tumorigenicity, and invasiveness. Accordingly, PKC $\epsilon$  up-regulation has been associated with poor disease-free and overall survival of breast cancer patients (22). More

\* This work was supported, in whole or in part, by National Institutes of Health Grant R01-CA89202 (to M. G. K.).

<sup>1</sup> To whom correspondence and reprints requests should be addressed: Dept. of Pharmacology, Perelman School of Medicine, University of Pennsylvania, 1256 Biomedical Research Bldg. IVIII, 421 Curie Blvd., Philadelphia, PA 19104-6160. Tel.: 215-898-0253; Fax: 215-746-8941; E-mail: marcelog@upenn.edu.

recently, a PKC $\epsilon$  ATP mimetic inhibitor was found to impair the growth of breast cancer cells *in vitro* and *in vivo*, highlighting the potential of PKC $\epsilon$  as a breast cancer therapeutic target (26). Regardless of the well accepted fact that dysregulation in PKC $\epsilon$  expression plays a causative role in cancer progression, little is known regarding the mechanisms that control the expression of this pro-oncogenic and metastatic kinase. To our knowledge, the transcriptional mechanisms controlling the expression of the *PRKCE* promoter in humans or other species have not yet been studied. To characterize the regulation of PKC $\epsilon$  expression, we cloned a fragment of the promoter region of the human *PRKCE* gene and investigated the critical determinants controlling transcriptional activation of this gene. Our analysis revealed key *cis*-acting elements in the *PRKCE* promoter and candidate transcription factors, particularly Sp1 and STAT1, that contribute to PKC $\epsilon$  overexpression in breast cancer. Furthermore, we identified a self-controlled mechanism that significantly contributes to the up-regulation of PKC $\epsilon$  in breast cancer cells.

## EXPERIMENTAL PROCEDURES

**Cell Culture**—Mammary (MCF-10A, MCF-7, T-47D, BT-474, HCC-1419, MDA-MB-231, MDA-MB-453, and MDA-MB-468), prostate (RWPE-1, LNCaP, C2, C2-4, DU145, and PC3), and lung (HBEC, H358, H1975, H1650, HCC827, PC9, H4006, H460, and A549) cell lines were purchased from the American Type Culture Collection (ATCC, Manassas, VA). PC3-ML cells were a kind gift of Dr. Alessandro Fatatis (Drexel University). Cancer cell lines were maintained in Dulbecco's modified Eagle's medium (DMEM) or RPMI 1640 medium supplemented with 10% FBS, L-glutamine (500  $\mu$ M), and penicillin/streptomycin (100 units/100  $\mu$ g/ml). Normal immortalized MCF-10A, HBEC, and RWPE-1 cells were cultured as described previously (18, 27). All cells were grown at 37 °C in a humidified 5% CO<sub>2</sub> incubator.

**Reagents**—The PKC inhibitor GF 109203X was purchased from Biomol (Plymouth Meeting, PA). Actinomycin D, mithramycin A, 5-aza-2'-deoxycytidine, and trichostatin A were obtained from Sigma.

**Cloning of the Human *PRKCE* Promoter and Generation of Luciferase Reporter Constructs**—All primers used for PCR were purchased from Integrated DNA Technologies (IDT, Coralville, IA). *PRKCE* promoter truncated fragments (−1933/+219, −1416/+219, −808/+219, −531/+219, −401/+219, −320/+219, and −105/+219) were amplified by PCR from human genomic DNA prepared from T-47D cells using BglII- and NheI-flanked following primers and subcloned into the pGL3-enhancer luciferase reporter vector (Promega, Madison, WI). The following were used: pGL3−1933/+219, CGTGCTAGCCAGACTTGACTTGGCAGAAG (forward) and TCGAGATCTGAAGGCCATTGAACACTACCATGGTTCG (reverse); pGL3−1416/+219, CGTGCTAGCCTCGCAGCCTGCGAAGTCCAGGACAG (forward) and TCGAGATCTGAAGGCCATTGAACACTACCATGGTTCG (reverse); pGL3−808/+219, CGTGCTAGCCTGACGTCTTTTGCAGATTTCCTGC (forward) and TCGAGATCTGAAGGCCATTGAACACTACCATGGTTCG (reverse); pGL3−531/+219, CGTGCTAGCGATGTGAGATTCCGGGCTCCT (forward) and

TCGAGATCTGAAGGCCATTGAACACTACCATGGTTCG (reverse); pGL3−401/+219, CGTGCTAGCACCATTTCCTCTCGACATGC (forward) and TCGAGATCTGAAGGCCATTGAACACTACCATGGTTCG (reverse); pGL3−320/+219, CGTGCTAGCCGCTGAGTGTGCGAAGAGGATCCG (forward) and TCGAGATCTGAAGGCCATTGAACACTACCATGGTTCG (reverse); and pGL3−105/+219, CGTGCTAGCCGACAGCTCGTCTTCTCTTCTGGAG (forward) and TCGAGATCTGAAGGCCATTGAACACTACCATGGTTCG (reverse). The pGL3−1416/+219 vector was used as a template to generate a series of *PRKCE* promoter truncated luciferase reporter vectors (−1319/+219, −1224/+219, −1121/+219, −1032/+219, −1028/+219, −921/+219, −887/+219, −873/+219, −819/+219, −796/+219, and −777/+219) with the Erase-a-Base kit (Promega, Madison, WI). pGL3−644/+219 was generated by digestion of pGL3−808/+219 vector with PflMI and NheI and subsequent religation. All constructs were verified by DNA sequencing.

**Site-directed mutagenesis**—For PCR-based mutagenesis, we used the QuikChange XL site-directed mutagenesis kit (Stratagene, La Jolla, CA). pGL3−921/+219 was used as a template to generate deletional mutations of STAT1 sites using the following primers: 1) CTATCGATCTCACTTCGTATTGCTCCCC (forward) and GGGGAGCAATACGAAAGTGAGATCGATAG (reverse); 2) GGCAAACTTTCTATCCCAACA-CTGCCG (forward) and CGGCAGTGTGGGATAGAAA-GTTTTGCC (reverse); 3) GACGTCTTTTGCAGTCTGCA-TTAGAGGGAG (forward) and CTCCCTCTAATGCAGATGCGCAAAAGACGTC (reverse); 4) CTCCGAGGAGGACC-ATCTCTCGACATGCATCCC (forward) and GGGATGCATGTCGAGAGATGGTCCTCCTCGGAG (reverse); and 5) CTCCCGGAGTCGAAATCCGGGATTATGTTTTCG (forward) and CGAAACATAATCCCGGATTTCGACTCCGGGAG (reverse). All mutant constructs were confirmed by DNA sequencing.

**Transient Transfection and Luciferase Assays**—Cells in 12-well plates ( $\sim 2 \times 10^5$  cells/well) were co-transfected with 450 ng of a *PRKCE* promoter Firefly luciferase reporter vector and 50 ng of the *Renilla* luciferase expression vector (pRL-TK) using Lipofectamine 2000 (Invitrogen) or X-tremeGENEHP DNA transfection reagent (Roche Applied Science). After 48 h, cells were lysed with passive lysis buffer (Promega, Madison, WI). Luciferase activity was determined in cell extracts using the Dual-Luciferase<sup>TM</sup> reporter assay kit (Promega). Data were expressed as the ratio between Firefly and *Renilla* luciferase activities. In each experiment, the pGL3-positive control vector (Promega) was used as a control. Promoter activity of each *PRKCE* promoter luciferase reporter construct was expressed as follows: (Firefly (sample)/*Renilla* (sample))/(Firefly (positive)/*Renilla* (positive))  $\times 100\%$ .

**Western Blot**—Western blot analysis was carried out essentially as described previously (28). Bands were visualized by the ECL Western blotting detection system. Images were captured using a FujiFILM LAS-3000 system. The following antibodies were used: anti-PKC $\epsilon$  and anti-Sp1 (1:1000, Santa Cruz Biotechnology Inc., Santa Cruz, CA); anti-STAT1 and anti-phospho-STAT1 (Ser-727) (1:1000, Cell Signaling Technology Inc., Danvers, MA); and anti-vinculin and anti- $\beta$ -actin (1:50,000,

Sigma). Anti-mouse or anti-rabbit conjugated with horseradish peroxidase (1:5000, Bio-Rad) was used as secondary antibodies.

**RNA Interference**—RNAi duplexes were transiently transfected using Lipofectamine RNAiMax. For transient depletion of PKC $\epsilon$ , STAT1, and Sp1, we used ON-TARGET Plus RNAi duplexes purchased from Dharmacon (Waltham, MA). Silencer control RNAi from Ambion was used as a nontarget control. Twenty four h after RNAi delivery, cells were transfected with different luciferase reporters, and luciferase activity was determined 48 h later.

**Real Time Quantitative PCR (qPCR)**<sup>2</sup>—Total RNA was extracted from subconfluent cell cultures using the RNeasy kit (Qiagen, Valencia, CA). One  $\mu$ g of RNA/sample was reverse-transcribed using the TaqMan reverse transcription reagent kit (Applied Biosystems, Branchburg, NJ) with random hexamers used as primers. PCR primers and a 5' end 6-carboxyfluorescein-labeled probe for PKC $\epsilon$  were purchased from Applied Biosystems. PCR was performed using an ABI PRISM 7700 detection system in a total volume of 25  $\mu$ l containing TaqMan universal PCR MasterMix (Applied Biosystems), commercial target primers (300 nM), the fluorescent probe (200 nM), and 1  $\mu$ l of cDNA. PCR product formation was continuously monitored using the sequence detection system software version 1.7 (Applied Biosystems). The 6-carboxyfluorescein signal was normalized to endogenous tRNA 18 S or ubiquitin C.  $\Delta$ Ct was obtained by subtracting the circle threshold (CT) of tRNA 18 S or ubiquitin C from that of PKC $\epsilon$ .  $\Delta(\Delta$ Ct) was determined by subtracting the control  $\Delta$ Ct from the sample  $\Delta$ Ct. Fold-changes were expressed as  $(2)^{-\Delta(\Delta$ Ct)}.

**RNA Stability Assay**— $5 \times 10^5$  cells seeded into 35-mm plates were treated with actinomycin D (2.5  $\mu$ g/ml) for 16 h. Total RNA from different cell lines was extracted at different times using TRIzol (Invitrogen). cDNA was synthesized using the TaqMan reverse transcription reagent kit (Applied Biosystems). PKC $\epsilon$  mRNA levels were determined by qPCR as described above. For each cell line, mRNA levels at time = 0 h was set as 100%.

**In Silico PKC $\epsilon$  mRNA Profiling in Breast Cancer Cells**—Analysis of PRKCE gene expression in breast cancer was done from three independent studies (GSE10843, GSE12777, and GSE41445) using inSilicoDb and inSilicoMerging R/Bioconductor packages (29). These gene expression profiles were developed using the Affymetrix HG-U133 Plus2 platform (GPL570). Briefly, the frozen RMA preprocessed expression profiles of these studies were downloaded from the InSilico database and merged using the COMBAT algorithm as the batch removal method. Visualization and statistical analysis of PKC $\epsilon$  expression profile were done with R.

**Analysis of Methylation of the PRKCE Promoter**—The presence of CpG islands in the human PRKCE promoter (NC\_000002.11) was determined using the Methyl Primer Express software (Applied Biosystems). For the analysis of PKC $\epsilon$  mRNA expression after demethylation, MCF-10A cells were treated with different concentrations (1–100  $\mu$ M) of 5-aza-2'-deoxycytidine (96 h or 7 days) and/or trichostatin A

(100 ng/ml, 24 h). Total mRNA was extracted, and PKC $\epsilon$  mRNA levels were determined by qPCR as described above.

**Electrophoretic Mobility Shift Assay (EMSA)**—EMSA was performed as described elsewhere (18). Briefly, nuclear and cytosolic fractions were obtained after cell lysis using the NE-PER nuclear protein extraction kit (Pierce). The following probes were used: STAT1-2 oligonucleotide probes (sense 5'-AGCTTTTCTATTTCCCCAAACACTGCCG-3' and antisense, 5'-AATTCCGGCAGTGTGGGGAAATAGAAA-3'); Sp1-2 oligonucleotide probe (sense 5'-AGCTTAGCGCGGAGGGCGGGCGCCGCGC-3' and antisense, 5'-AATTCGCGCCGGCGCCCGCCCTCCGCGCT-3'); STAT1 consensus probe (sense, 5'-AGCTTCATGTTATGCATATTCCTGTAAGTG and antisense, 5'-AATTCCACTTACAGGAATATGCATAACATG-3'); Sp1 consensus probe (sense, 5'-AGCTTATTCGATCGGGGCGGGGCGAGC-3' and antisense, 5'-AATTCGCTCGCCCCGCCCGATCGAAT-3'). Probes were labeled with [ $\alpha$ -<sup>32</sup>P]deoxyadenosine triphosphate using Klenow enzyme and purified on a Sephadex G-25 column. The binding reaction was carried out at 25 °C for 10 min with or without nuclear proteins (5  $\mu$ g), poly(dI-dC) (1  $\mu$ g), and labeled probe (10<sup>6</sup> cpm) in 20  $\mu$ l of binding buffer (10 $\times$  buffer: 100 mM Tris-HCl, pH 7.5, 500 mM NaCl, 50 mM MgCl<sub>2</sub>, 100 mM EDTA, 10 mM DTT, 1% Triton X-100, and 50% glycerol). Binding specificity was confirmed by cold competition with 50-fold molar excess of cold STAT1 or Sp1 oligonucleotides. Cold AP-1 oligonucleotides (AP-1 sense 5'-AGCTTCGCTTGATGACTCAGCCGGAA-3' and antisense 5'-AATTCTTCCGGCTGAGTCATCAAGCG-3') were used as negative controls. DNA-protein complexes were separated on a 6% nondenaturing polyacrylamide gel at 200 V. The gel was fixed and dried, and DNA-protein complexes were visualized by autoradiography.

**Chromatin Immunoprecipitation (ChIP) Assay**—ChIP assay was performed essentially as described previously (30). Briefly,  $2 \times 10^6$  cells were fixed in 1% formaldehyde for 15 min to cross-link DNA with associated proteins. The cross-linking reaction was terminated by the addition of 125 mM glycine, and cells were then washed and harvested in PBS containing protease/phosphatase inhibitors. The pelleted cells were lysed on ice in a buffer containing 50 mM Tris-HCl, pH 8.1, 1% SDS, 10 mM EDTA, and protease/phosphatase inhibitors. Cells were sonicated for 10 s (six times). DNA was fragmented in a range of 200–1000 bp. Equal amounts of chromatin were diluted in ChIP buffer (16.7 mM Tris-HCl, pH 8.1, 0.01% SDS, 1.1% Triton X-100, 1.2 mM EDTA, and 167 mM NaCl) and incubated overnight at 4 °C with anti-STAT1 or anti-Sp1 antibodies (Abcam, Cambridge, MA) or control rabbit IgG (Cell Signaling Inc.), followed by 1 h of incubation with salmon sperm DNA/protein A-agarose beads. 10% of the sample was kept as input. Protein A-agarose beads pellets were sequentially washed with a low salt buffer (20 mM Tris-HCl, pH 8.1, 0.1% SDS, 1% Triton X-100, 2 mM EDTA, and 150 mM NaCl), a high salt buffer (20 mM Tris-HCl, pH 8.1, 0.1% SDS, 1% Triton X-100, 2 mM EDTA, and 500 mM NaCl), LiCl wash buffer (10 mM Tris-HCl, pH 8.1, 0.25 M LiCl, 1% Nonidet P-40, 1% deoxycholate, 1 mM EDTA), and TE buffer (10 mM Tris-HCl, pH 8.0, and 1 mM EDTA). Protein-DNA complexes were eluted in a buffer containing 1% SDS and 0.1 M NaHCO<sub>3</sub>. Cross-linking was reversed with 200

<sup>2</sup> The abbreviations used are: qPCR, quantitative PCR; MTM, mithramycin A; AZA, 5-aza-2'-deoxycytidine.



mM NaCl overnight at 65 °C, followed by incubation in a buffer containing 40 mM Tris-HCl, pH 6.5, 10 mM EDTA, and 20  $\mu$ g of proteinase K for 2 h at 55 °C. DNA was then extracted with QIAquick PCR purification kit (Qiagen) and analyzed by PCR. For STAT1-2/3 sites –880/–869 and –793/782 bp, we used primers 5'-CGCCAGCTCTCCACCGTTGTC (forward) and 5'-GTCGGTGTGCGAGCGAGTCTCC (reverse). For Sp1-2 site –668/–659 bp, we used primers 5'-GGAGACTCGCTCGCACACCGAC (forward) and 5'-GCAGGGACTGCGACTCAGCG (reverse). For Sp1-5 site –347/–338 bp, we used primers 5'-GTGGGGCTTGTGGATTTTTA (forward) and 5'-AGATTTCAACCCGGATCCTC (reverse). For Sp1-6/7 sites –269/–260 bp and –256/–247 bp, we used primers 5'-CGCTGAGTGTGCGAAGAGGATCC (forward) and 5'-CCGGC-GCTTACCTACCTTTCCG (reverse).

**Cell Migration Assay**—Cell migration was determined with a Boyden chamber, as described previously (31). Briefly, MCF-7 cells ( $3 \times 10^4$  cells/well) were seeded in the upper compartment of a Boyden chamber (NeuroProbe). A 12- $\mu$ m pore polycarbonate filter (NeuroProbe) coated overnight with type IV collagen in cold PBS was used to separate the upper and lower compartments. In the lower chamber, 0.1% BSA/DMEM with or without FBS (5%) was used. After 24 h of incubation at 37 °C, nonmigrating cells on the upper side of the membrane were wiped off the surface, and migrating cells on the lower side of the membrane were fixed, stained with DIFF Quik Stain Set (Dade Behring), and counted by contrast microscopy in five independent fields.

**Statistical Analysis**—Results are the means  $\pm$  S.E. of at least three individual experiments. Student's *t* test was used for statistical comparison. A *p* value < 0.05 was considered statistically significant.

## RESULTS

**Overexpression of PKC $\epsilon$  in Breast Cancer Cells and Initial Characterization of the PRKCE Promoter**—PKC $\epsilon$ , a kinase broadly implicated in tumorigenesis and metastasis, is overexpressed in multiple cancers. Elevated PKC $\epsilon$  levels have been associated with poor outcome in prostate, breast, lung, and head and neck cancer (22, 24, 32, 33); however, the mechanisms behind the control of PKC $\epsilon$  expression remain to be established. A comparative analysis of PKC $\epsilon$  protein levels by Western blot shows that this kinase is overexpressed in multiple breast cancer cell lines (MCF-7, T-47D, BT-474, HCC-1419, MDA-MB-231, MDA-MB-453, and MDA-MB-468 cells) relative to MCF-10A cells, an immortalized nontumorigenic mammary cell line (Fig. 1A). qPCR assays also revealed significantly higher PKC $\epsilon$  mRNA levels in breast cancer cells compared with MCF-10A cells (Fig. 1B). To determine whether overexpression of PKC $\epsilon$  is associated with altered mRNA stability, we assessed mRNA levels at different times after treatment with the transcriptional inhibitor actinomycin D. As shown in Fig. 1C, the decay in mRNA levels is essentially the same in breast cancer cell lines (MCF-7, T-47D, and MDA-MB-453) and MCF-10A cells. Thus, the differential expression of PKC $\epsilon$  may involve a dysregulation of transcriptional mechanisms. Likewise, and in agreement with previous studies (18, 27), PKC $\epsilon$  is overexpressed in lung and prostate cancer cell lines relative to corresponding normal “nontransformed” cell lines (Fig. 1A).

To investigate the transcriptional mechanisms involved in PKC $\epsilon$  expression, we cloned a 2.1-kb fragment of the human *PRKCE* gene from genomic DNA using PCR. This fragment includes 1933 bp of the putative *PRKCE* promoter as well as 219 bp after the putative transcription start site. We also cloned four fragments encompassing shorter regions of the putative *PRKCE* promoter (1416/+219 bp, 808/+219 bp, 320/+219 bp, and 105/+219 bp, respectively). The different DNA fragments were subcloned into the pGL3-enhancer luciferase reporter vector to generate the plasmids pGL3–1933/+219, pGL3–1416/+219, pGL3–808/+219, pGL3–320/+219, and pGL3–105/+219. Plasmids were transiently transfected into MCF-7 breast cancer cells along with pRL-TK (*Renilla* luciferase vector) for normalization of transfection efficiency. The pGL3–1416/+219 reporter construct exhibited the highest luciferase activity, which was  $\sim$ 40 times higher than pGL3-enhancer empty vector, therefore confirming that it possesses functional *PRKCE* promoter activity. A progressive loss in luciferase activity was observed upon deletions of fragments –1416/–809, –1416/–321, and –1416/–106. A significant loss of promoter activity was also observed with pGL3–1933/+219, suggesting repressive transcriptional elements within the –1933/–1417 bp region (Fig. 1D). A comparison of *PRKCE* promoter activity in different cell lines using pGL3–1416/+219 revealed a manifest elevation in luciferase activity in breast cancer cells relative to normal immortalized MCF-10A cells. Similarly, lung and prostate cancer cell lines exhibited higher promoter activity than the corresponding nontumorigenic counterparts (Fig. 1E).

A comparative analysis of *PRKCE* gene expression in 48 breast cancer cell lines (24 luminal-like and 24 basal-like) obtained from three independent studies (GSE10843, GSE12777, and GSE41445) was performed using inSilicoDb and inSilicoMerging R/Bioconductor packages (29). This analysis showed no statistically significant differences between luminal and basal-like breast cancer cell lines (*p* = 0.673) (Fig. 1F).

**Differential Expression of PKC $\epsilon$  Is Not Related to Promoter Methylation**—It is well established that epigenetic mechanisms control the expression of key oncogenic and tumor-suppressing proteins. To determine whether methylation of the *PRKCE* promoter could be implicated in the differential expression between normal mammary and breast cancer cells, we first examined if the promoter was rich in CpG islands using the Methyl Primer Express software (Applied Biosystems). This analysis revealed two regions in the *PRKCE* promoter that were very rich in CpG islands, a proximal region between –2.6 and +0.9 kb and a distal region between –8.9 and –7.7 kb (Fig. 2A). To determine whether the reduced PKC $\epsilon$  expression in MCF-10A cells could be due to promoter methylation, we used the demethylating agent 5-aza-2'-deoxycytidine (AZA). qPCR analysis revealed that PKC $\epsilon$  mRNA levels remain essentially unchanged in MCF-10A cells treated with different concentrations of AZA, either in the presence or absence of the HDAC inhibitor trichostatin A (Fig. 2B). A similar treatment in MCF-10A cells caused a significant rescue in the expression of the oncogenic protein P-Rex1, a gene that is regulated by methyl-

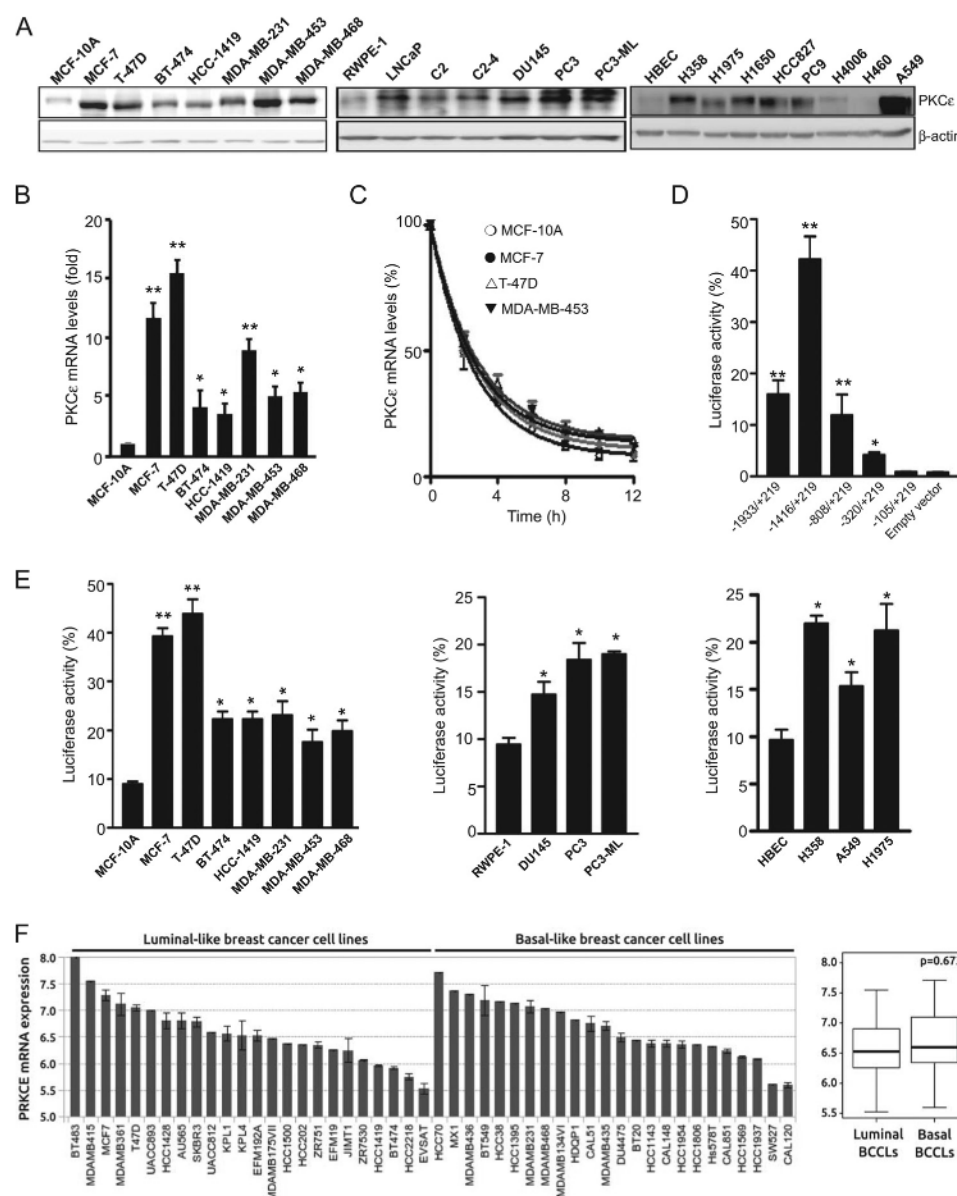


**FIGURE 1. Elevated PKC $\epsilon$  expression and PRKCE promoter activity in breast cancer cells.** A, PKC $\epsilon$  expression in immortalized "normal" MCF-10A mammary epithelial cells, RWPE-1 prostate epithelial cells, and HBEC lung epithelial cells, as well as in breast, prostate, and lung cancer cell lines, as determined by Western blot. Similar results were observed in three independent experiments. B, PKC $\epsilon$  mRNA levels in mammary cell lines, as determined by qPCR. Data are expressed as mean  $\pm$  S.E. of three independent experiments. \*,  $p < 0.05$ ; \*\*,  $p < 0.01$  versus MCF-10A cells. C, PKC $\epsilon$  mRNA stability in MCF-10A, MCF-7, T-47D, and MDA-MB-453 cell lines. Cells were treated with actinomycin D (2.5  $\mu$ g/ml), and RNA was extracted at different times. PKC $\epsilon$  mRNA levels were measured by qPCR. Data are expressed as percentage relative to levels at  $t = 0$  and represent the mean  $\pm$  S.E. of three independent experiments. D, analysis of PRKCE promoter activity. Luciferase reporter plasmids pGL3-1933/+219, pGL3-1416/+219, pGL3-808/+219, pGL3-320/+219, pGL3-105/+219, and pGL3 empty vector were transfected into MCF-7 cells along with the pRL-TK Renilla luciferase vector. Luciferase activity was determined 48 h later. Data are expressed as mean  $\pm$  S.E. of three independent experiments. \*,  $p < 0.05$ ; \*\*,  $p < 0.01$  versus pGL3 vector. E, luciferase activity in normal and cancer cells was determined 48 h after transfection of different cell lines with pGL3-1416/+219 along with the pRL-TK Renilla luciferase vector. Data are expressed as mean  $\pm$  S.E. of three independent experiments. \*,  $p < 0.05$ ; \*\*,  $p < 0.01$  versus nontumorigenic cells. F, PKC $\epsilon$  expression profile based on a compiled dataset of breast cancer cell lines (BCCLs) (left panel), which show no significant statistical differences between those of luminal and basal origin ( $p = 0.673$ ) (right panel).

tion.<sup>3</sup> Therefore, overexpression of PKC $\epsilon$  in breast cancer cells does not seem to be related to demethylation of the PRKCE gene promoter.

**Identification of Key Transcriptional Regions in the Human PKC $\epsilon$  Promoter**—To characterize the human PRKCE promoter in more detail and to identify positive regulatory elements

responsible for transcriptional activation, a series of 5'-unidirectional deletions was generated from the pGL3-1416/+219 luciferase reporter vector using the Erase-a-Base system. The resulting constructs were transfected into MCF-7 cells, and luciferase activity was determined. Fig. 3 shows that promoter activities of pGL3-1319/+219, pGL3-1224/+219, pGL3-1121/+219, pGL3-1032/+219, pGL3-1028/+219, and pGL3-921/+219 constructs were essentially similar to that of pGL3-1416/+219. However, a significant

<sup>3</sup> L. Barrio-Real, L. G. Benedetti, N. Engel, Y. Tu, S. Cho, S. Sukumar, and M. G. Kazanietz, in press.

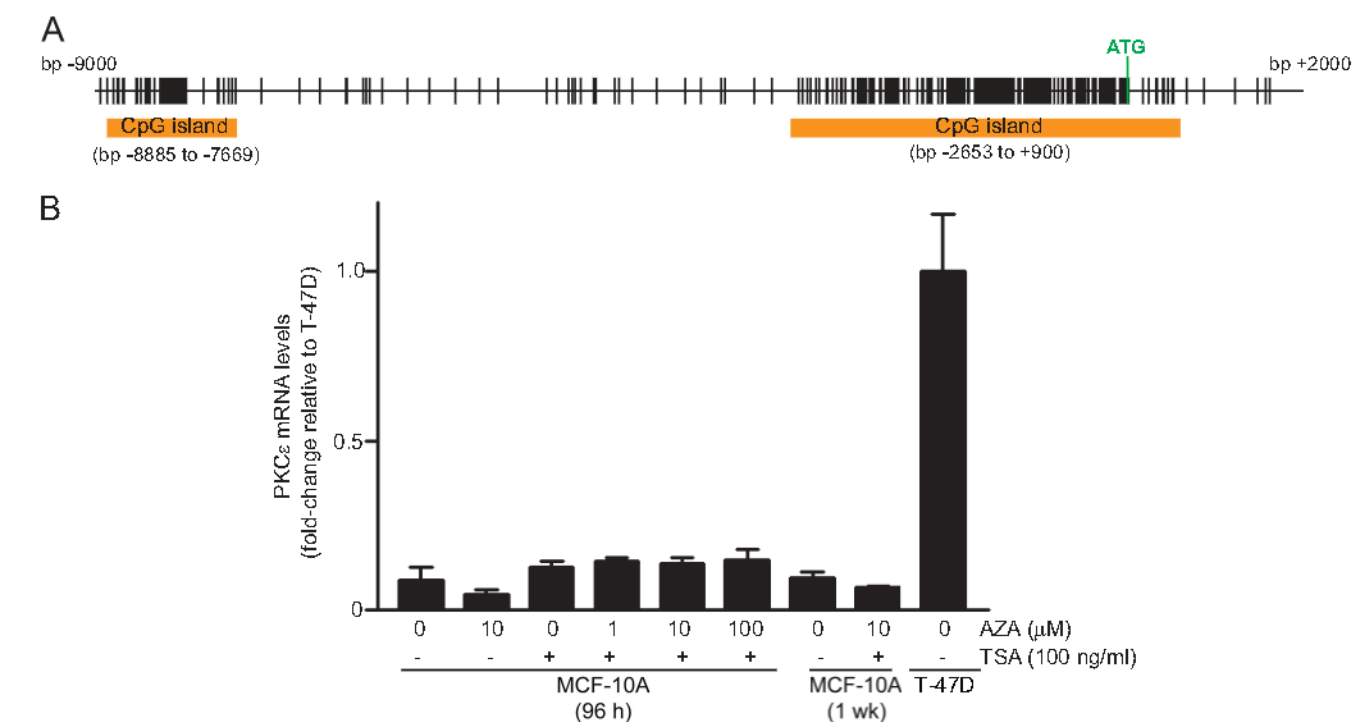


**FIGURE 2. Methylation of *PRKCE* promoter is not associated with low PKC $\epsilon$  mRNA levels in MCF-10A cells.** *A*, identification of CpG islands in the *PRKCE* promoter with the Methyl Primer Express software (Applied Biosystems). *B*, MCF-10A cells were treated with different concentrations of AZA (1–100  $\mu$ M, 96 h or 1 week), trichostatin A (TSA, 100 ng/ml, 24 h), or a combination of both drugs. At the end of the treatment, total RNA was isolated, and PKC $\epsilon$  mRNA levels were determined by qPCR. For comparison, PKC $\epsilon$  mRNA levels were also measured in T-47D cells. Data are expressed as fold-change relative to levels in T-47D cells (mean  $\pm$  S.D.,  $n = 3$ ). Similar results were observed in two independent experiments.

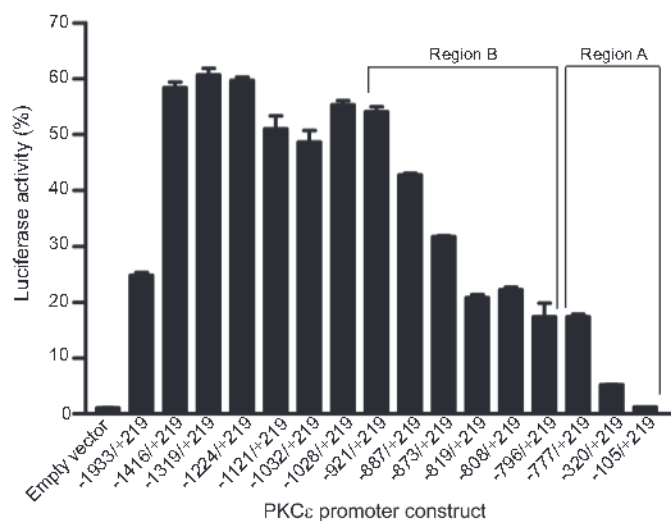


**FIGURE 3. Deletional analysis of the human *PRKCE* promoter.** MCF-7 cells were co-transfected with pGL3 vectors coding different PKC $\epsilon$  promoter fragments generated with the Erase-a-Base kit (Promega) and pRL-TK plasmid. Luciferase activity was measured 48 h later. Data are expressed as mean  $\pm$  S.D. of triplicate samples. Two additional experiments gave similar results.

reduction in transcriptional activity was observed upon serial deletions starting from bp -887. Indeed, pGL3-887/+219, pGL3-873/+219, and pGL3-819/+219 display 77, 58, and 37% activity, respectively, compared with that of pGL3-1416/+219. No additional changes in reporter activity were observed with pGL3-808/+219. Constructs pGL3-796/+219 and pGL3-777/+219 display slightly lower luciferase activity than pGL3-808/+219. Luciferase activity drops significantly with constructs pGL3-320/+219 (91% reduction) and pGL3-105/+219

(98% reduction). To summarize these initial observations, the deletional analysis delineated two prominent regions in the *PRKCE* promoter containing positive regulatory elements that we defined as region A (-777 to -105 bp) and region B (-921 to -796 bp). In subsequent sections, a more detailed characterization of the *cis*-acting elements in these two regions will be shown.

**Analysis of Region A Revealed a Crucial Role for Sp1 in PKC $\epsilon$  Transcription**—To identify putative transcriptional elements in region A of the *PRKCE* promoter, we initially used the PROMO software. This analysis revealed the presence of seven putative Sp1-responsive elements that we named Sp1-1 (the most distal site, bp -716 to -707) to Sp1-7 (the most proximal site, bp -256 to -247) (Fig. 4A, left panel). The putative Sp1-binding sequences are shown in Fig. 4A, right panel. To define the relevance of the different Sp1-binding sites, additional truncated mutants for region A were generated using pGL3-777/+219 as a template (pGL3-644/+219, pGL3-531/+219, and pGL3-401/+219), and we examined for their luciferase activity upon transfection into MCF-7 cells. Fig. 4B shows that deletion of region comprising bp -777 to -664 (which includes Sp1-1 and Sp1-2 sites) caused a 65% drop in luciferase activity. No additional changes in reporter activity were observed upon deletions of regions comprising bp -644/-532, -644/-402, and -644/-321, which include sites Sp1-3, Sp1-4, and Sp1-5. However, when fragment -320/-105 (which includes Sp1-6 and Sp1-7) was deleted, an additional reduction in luciferase activity was observed. These results suggest that multiple Sp1 sites in region A contribute to the transcriptional activity of the *PRKCE* promoter.

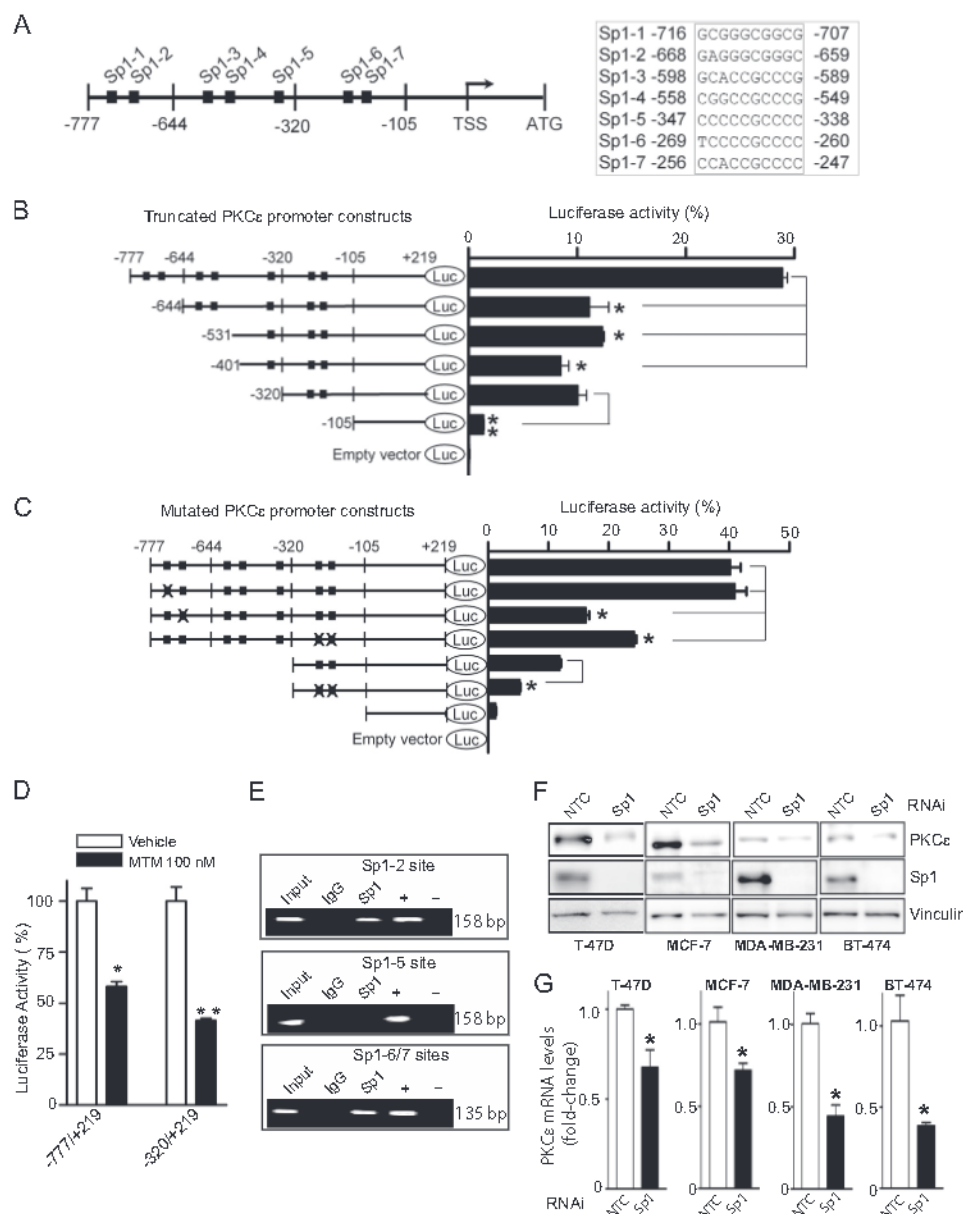


**FIGURE 4. Sp1 elements in region A of the *PRKCE* promoter control its transcriptional activity.** *A*, schematic representation of putative Sp1 sites (black boxes) in the *PRKCE* gene promoter. Seven putative Sp1-binding sites (Sp1-1 through Sp1-7) were identified (left panel). The corresponding sequences are shown (right panel). TSS, putative transcription starting site; ATG, start codon. *B*, deletion analysis of region A. Luciferase (Luc) activity of truncated constructs was determined 48 h after transfection into MCF-7 cells. Data are expressed as mean  $\pm$  S.D. of triplicate samples. Two additional experiments gave similar results. \*,  $p < 0.05$ ; \*\*,  $p < 0.01$  versus control vector. *C*, schematic representation of mutated *PRKCE* promoter reporter constructs. The nonmutated Sp1 sites are indicated with black square boxes, and the mutated sites are marked with X on the black box. Luciferase activity of truncated constructs was determined 48 h after transfection into MCF-7 cells. Data are expressed as mean  $\pm$  S.D. of triplicate samples. Two additional experiments gave similar results. \*,  $p < 0.05$  versus wild-type vector. *D*, MCF-7 cells were transfected with pGL3-777/+219 or pGL3-320/+219 reporter vectors and 24 h later treated with the Sp1 inhibitor mithramycin A (MTM, 100 nM) or vehicle for 16 h. Data are expressed as mean  $\pm$  S.D. of triplicate samples. Two additional experiments gave similar results. \*,  $p < 0.05$ ; \*\*,  $p < 0.01$  versus control. *E*, ChIP assay. Upper panel, ChIP assay for Sp1-2 sites (fragment comprising bp -668/-659). Middle panel, ChIP assay for Sp1-5 site (fragment comprising bp -347/-338). Lower panel, ChIP assay for Sp1-6/7 sites (fragment comprising bp -269/-260 and bp -256/-247). *F*, MCF-7, T-47D, MDA-MB-231, and BT-474 cells were transiently transfected with Sp1 or nontarget control (NTC) RNAi duplexes. PKC $\epsilon$  expression was determined by Western blot after 72 h. *G*, PKC $\epsilon$  mRNA expression was determined by qPCR 72 h after transfection with either Sp1 or nontarget control RNAi duplexes. Data are expressed as fold-change relative to nontarget control and represent the mean  $\pm$  S.D. of triplicate samples. \*,  $p < 0.05$  versus control. Similar results were observed in two independent experiments.

To further determine the contribution of the different Sp1 sites in the transcriptional activation of the *PRKCE* promoter, we performed site-directed mutagenesis of these sites in the context of the pGL3-777/+219 construct. Essential residues GGCG in Sp1 sites were mutated to TTAT, and luciferase activities of the corresponding constructs were determined after transfection into MCF-7 cells. As shown in Fig. 4C, mutation

of Sp1-1 in pGL-777/+219 had no effect; however, mutation of Sp1-2 caused a 62% reduction in reporter activity. Sp1-6 and Sp1-7 were only 4 bp apart, and therefore we decided to mutate them together. When we mutated Sp1-6/7 in pGL3-777/+219, a significant reduction (50%) in luciferase activity was observed. We further mutated Sp1-6/7 sites in pGL3-320/+219, and observed a significant reduction in reporter activity



compared with the wild-type pGL3-320/+219 construct. However, it did not reach complete inhibition, thus arguing for the presence of other relevant transcriptional element(s) within the -320/-105 region that remain to be identified. The deletion and mutational analyses of region A indicate that multiple Sp1 sites control the transcriptional activation of the *PRKCE* promoter.

To confirm the relevance of the Sp1-binding sites in transcriptional activation of the *PRKCE* gene, we used a number of additional approaches. First, we examined the effect of mithramycin A (MTM), an agent that prevents binding of Sp1 to its transcription binding site (34, 35). As shown in Fig. 4D, MTM markedly reduced luciferase activity of reporters pGL3-777/+219 and pGL3-320/+219. As a second approach, and to address whether Sp1 proteins associate with the *PRKCE* promoter *in vivo*, we performed a chromatin immunoprecipitation (ChIP) assay using an anti-Sp1 antibody. As a negative control, we used IgG. Three sets of primers were utilized in these experiments as follows: one encompassing bp -772 to -615 (for site Sp1-2); a second encompassing bp -320 to -186 (for Sp1-6 and Sp1-7), and a third for bp -443 to -286 (for site Sp1-5). Sp1 immunoprecipitation revealed the expected bands for regions -772/-615 and -320/-186, and no band was observed for region -443/-286 (Fig. 4E). Thus, the Sp1 transcription factor binds *in vivo* to the sites identified in our deletion/mutational analysis. Finally, to confirm the involvement of Sp1, we knocked down this transcription factor using RNAi. Sp1 RNAi depletion from MCF-7, T-47D, MDA-MB-231, and BT-474 breast cancer cell lines significantly reduced the expression of PKC $\epsilon$  protein (Fig. 4F) and PKC $\epsilon$  mRNA, as determined by qPCR (Fig. 4G). Altogether, these results demonstrate the relevance of Sp1 in transcriptional activation of the *PRKCE* promoter.

**STAT1-binding Sites in Region B Control PKC $\epsilon$  Transcriptional Activation**—As established in the deletion analysis shown in Fig. 3, region B located between bp -921 and -796 plays a positive role in transcriptional activation of the *PRKCE* promoter. Analysis using the PROMO program revealed two putative STAT1 sites in this region, which we named STAT1-1 (-916 to -905 bp) and STAT1-2 (-880 to -869 bp). There is also a third STAT1 site (STAT1-3) at the edge of region B (-793 to -782 bp) (Fig. 5A). To determine the potential relevance of these sites, essential residues TTTCC in STAT1 sites were mutated to T→C in pGL3-921/+219. The resulting mutant constructs were transfected into MCF-7 cells and assessed for their luciferase reporter activity. As shown in Fig. 5B, mutation of the most distal STAT1 site (STAT1-1) had no significant effect on luciferase activity. Conversely, mutation of STAT1-2 site caused a 44% reduction in reporter activity. A slight, yet statistically significant reduction in luciferase activity was observed upon mutation of the STAT1-3 site. A double mutant for STAT1-2 and STAT1-3 sites was generated, and its activity was examined in MCF-7 cells, which revealed a 61% reduction in luciferase activity compared with the pGL3-921/+219 construct. Therefore, the STAT1-2 and STAT1-3 sites are involved in the regulation of PKC $\epsilon$  promoter activity.

The program PROMO also identified two additional STAT1 sites outside region B, which were named STAT1-4 (-401 to

-390bp) and STAT-5 (-227 to -216 bp). These two sites were actually located within the region A and in close proximity to Sp1 sites (Fig. 5A). We mutated STAT1-4 and STAT1-5 sites and found these mutations do not alter reporter activity (Fig. 5B), suggesting that only STAT1-2 and STAT1-3 sites are involved in transcriptional control of the *PRKCE* promoter in breast cancer cells.

Next, to confirm the relevance of STAT1 in the control of PKC $\epsilon$  transcriptional activity, we used RNAi (Fig. 5C). MCF-7 cells were transfected with a STAT1 SMARTpool®RNAi, which caused >90% depletion in STAT1 levels (Fig. 5C, inset), or a SMARTpool® control RNAi and then transfected with the pGL3-921/+219 luciferase reporter vector. As expected from the deletion and mutational analyses, silencing STAT1 inhibited transcriptional activity of the PKC $\epsilon$  reporter (54% reduction, which is in the same range as the reduction in activity observed upon mutation of STAT1-2 and STAT1-3 sites combined, see Fig. 5B). Moreover, when we assessed the activity of the STAT1-2/3-mutated pGL3-921/+219 construct, STAT1 RNAi depletion failed to cause an additional reduction in luciferase activity (Fig. 5C), thus confirming the importance of STAT1-2 and STAT1-3 sites in the control of *PRKCE* promoter activity. To further confirm the relevance of the STAT1 sites, we used ChIP. For this analysis, we used a set of primers encompassing -949 to -751 bp in the *PRKCE* promoter, a region that includes both STAT1-2- and STAT1-3-binding sites. Results shown in Fig. 5D revealed a band of the expected size (199 bp) when an anti-STAT1 antibody was used in the immunoprecipitation, whereas no band was observed using control IgG, thus suggesting direct binding of STAT1 to the -949 to -751-bp promoter region. Furthermore, STAT1 RNAi depletion from MCF-7 cells caused a significant reduction in PKC $\epsilon$  mRNA (Fig. 5E) and protein levels (Fig. 5F). Altogether, these results indicate that STAT1-2- and STAT1-3-binding sites are involved in the transcriptional control of the *PRKCE* promoter. An additive effect between STAT1 RNAi depletion and MTM treatment was observed (Fig. 5F).

**STAT1 and Sp1 Contribute to the Elevated PKC $\epsilon$  Transcriptional Activity in Breast Cancer Cells**—Once we identified relevant Sp1 and STAT1 sites in the *PRKCE* promoter, we asked if these sites mediate PKC $\epsilon$  up-regulation in breast cancer cells relative to nontumorigenic mammary cells. To address this issue, we compared the activities of the different deleted reporters between MCF-7 versus MCF-10A cells. As shown previously in Fig. 1E with reporter pGL3-1416/+219, activity of pGL3-921/+219 reporter was also higher in MCF-7 cells relative to MCF-10A cells (Fig. 6A). Deletion of fragment -921 to -777 bp, which includes STAT1-2/3 sites in region B, diminished luciferase activity in MCF-7 cells by 61%, an effect that was not seen in MCF-10A cells (Fig. 6, A and B). To verify the relevance of the STAT1 sites in PKC $\epsilon$  up-regulation in breast cancer cells, we compared the activity of pGL3-921/+219 (wild type) versus pGL3-921/+219 (STAT-2/3-mutated) in MCF-7 and MCF-10A cells. Whereas mutation of STAT1-2 and STAT1-3 sites failed to reduce reporter activity in MCF-10A cells, a marked reduction in activity (~70% reduction) was observed in MCF-7 cells (Fig. 6C) as well as in T-47D cells (data not shown). To validate the relevance of the STAT1-2/3 sites in



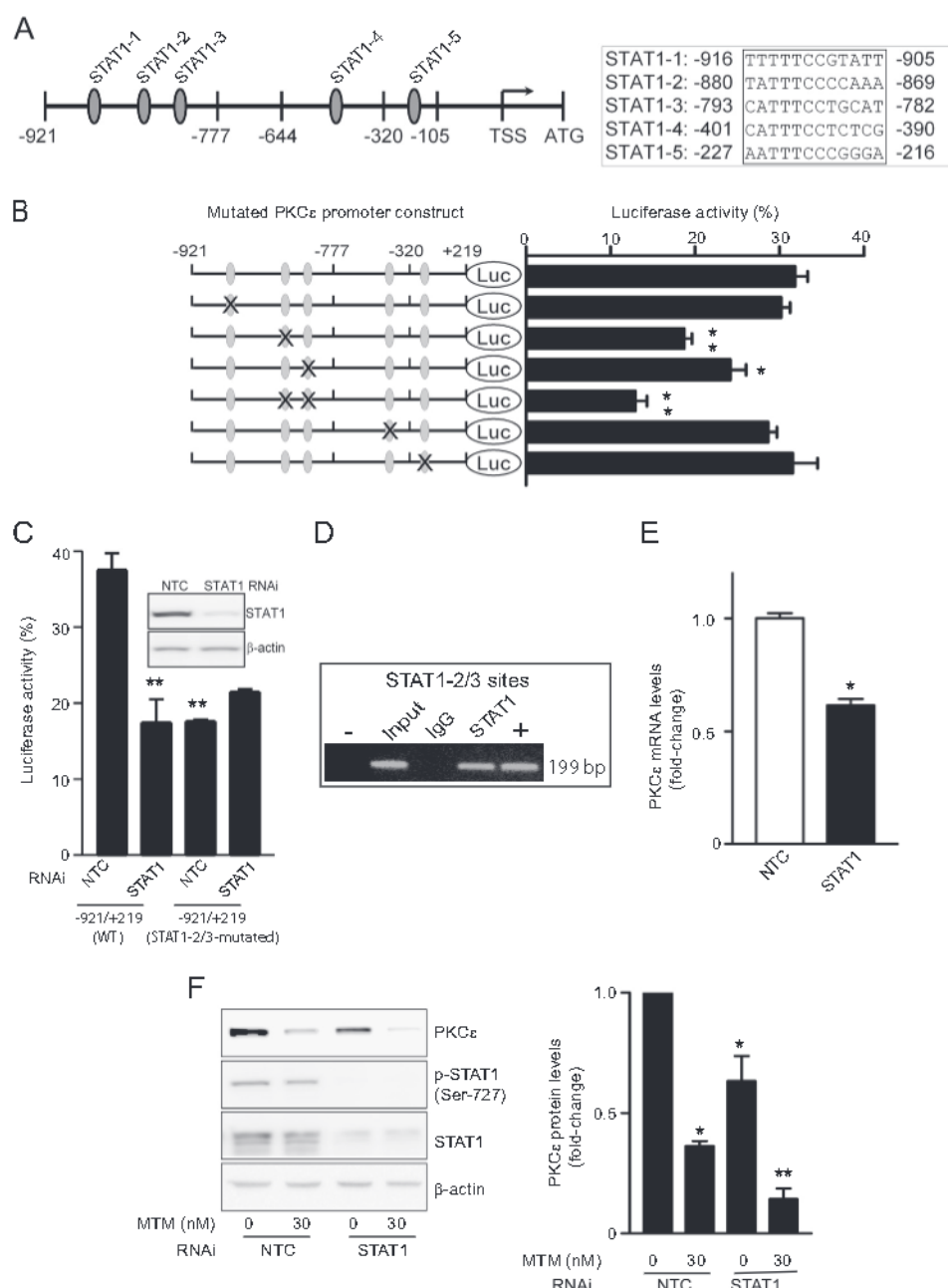


**FIGURE 5. STAT1 elements in region B of the *PRKCE* promoter control its transcriptional activity.** *A*, schematic representation of putative STAT1 sites (gray ovals) in the *PRKCE* gene promoter. Five putative STAT1-binding sites (STAT1-1 through STAT1-5) were identified (left panel). The corresponding sequences are shown (right panel). TSS, putative transcription starting site. ATG, start codon. *B*, schematic representation of mutated PKC $\epsilon$  promoter reporter constructs. The nonmutated STAT1 sites are indicated with gray ovals, and the mutated sites are marked with X on the gray oval. Luciferase (Luc) activity of mutated constructs was determined 48 h after transfection into MCF-7 cells. Data are expressed as mean  $\pm$  S.D. of triplicate samples. Two additional experiments gave similar results. \*,  $p < 0.05$ ; \*\*,  $p < 0.01$  versus pGL3-921/+219 (WT). *C*, STAT1 RNAi depletion inhibits luciferase activity of wild-type pGL3-921/+219 but not pGL3-921/219 (STAT1 2/3 mutated) construct. MCF-7 cells were transiently transfected with STAT1 or nontarget control (NTC) RNAi duplexes. Luciferase activity was determined 48 h after transfection of luciferase reporters. Inset, STAT1 expression as determined by Western blot. Data are expressed as mean  $\pm$  S.D. of triplicate samples. Two additional experiments gave similar results. \*,  $p < 0.05$ ; \*\*,  $p < 0.01$  versus pGL3-921/+219 (WT). *D*, ChIP assay for STAT1-2 and STAT1-3 sites (fragment comprising bp -880/-869 and bp -793/-782). *E*, PKC $\epsilon$  mRNA expression was determined by qPCR 72 h after transfection with either STAT1 or nontarget control RNAi duplexes. Data are expressed as fold-change relative to nontarget control and represent the mean  $\pm$  S.D. of triplicate samples. \*,  $p < 0.05$  versus control. Similar results were observed in two independent experiments. *F*, effect of combined STAT1 RNAi depletion and treatment with the Sp1 inhibitor MTM (30 nM for 48 h). PKC $\epsilon$  expression was determined by Western blot 72 h after RNAi duplex transfection (left panel). A densitometric analysis of four individual experiments is also shown (right panel). Results, normalized to control (NTC, no MTM treatment) are expressed as mean  $\pm$  S.E. \*,  $p < 0.05$ ; \*\*,  $p < 0.01$  versus control.

PKC $\epsilon$  up-regulation, we used an EMSA approach. Nuclear extracts from MCF-10A, MCF-7, or T-47D cells were incubated with 25-bp double-stranded radiolabeled probes for either the STAT1-2 site or a standard STAT1 binding consensus. As shown in Fig. 6D, a shift protein-DNA complex band

was detected after incubation of nuclear extracts from either probe both in MCF-7 (lanes 3 and 6) and T-47D cells (lanes 4 and 7). However, this effect was not seen in nontumorigenic MCF-10A cells (Fig. 6D, lanes 2 and 5). The shift band was competed by co-incubation with an excess (50-fold molar) of

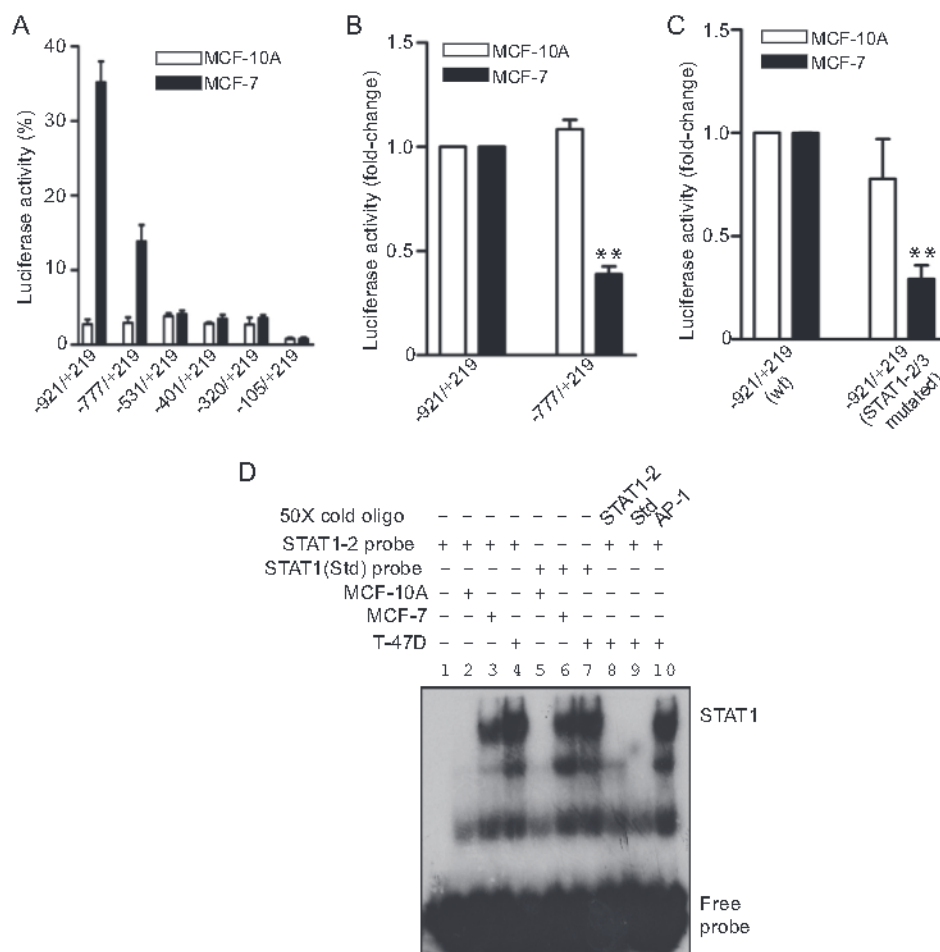


**FIGURE 6. Contribution of STAT1-2 and STAT1-3 sites to PKC $\epsilon$  overexpression in breast cancer cells.** *A*, cells were co-transfected with the indicated constructs together with the pRL-TK-Renilla luciferase plasmid. Luciferase activity was determined 48 h after transfection. Data are expressed as the mean  $\pm$  S.E. of three independent experiments. *B*, deletion of region comprising sites STAT-2 and STAT-3 decreases PKC $\epsilon$  promoter activity in MCF-7 breast cancer cells but not in MCF-10A cells. Luciferase activities of constructs pGL3-921/+219 and pGL3-777/+219 were determined 48 h after transfection. Data are expressed as mean  $\pm$  S.E. of three individual experiments. Activity of pGL3-921/+219 was set as 1. \*\*,  $p < 0.01$  versus pGL3-921/+219. *C*, mutation of STAT-2 and STAT-3 sites reduces PKC $\epsilon$  promoter activity in MCF-7 breast cancer cells but not in MCF-10A cells, as determined 48 h after transfection of indicated plasmids. Data are expressed as mean  $\pm$  S.E. of three individual experiments. Luciferase activity of wild-type pGL3-921/+219 was set as 1. \*\*,  $p < 0.01$  versus pGL3-921/+219 (WT). *D*, elevated STAT-DNA binding activity in MCF-7 and T-47D breast cancer cells, as determined by EMSA. Similar results were observed in three independent experiments.

unlabeled probes for either STAT1-2 (Fig. 6D, lane 8) or a standard STAT1-binding consensus sequence (lane 9) but not with an excess unlabeled probe for AP-1 (lane 10), thereby confirming the specificity of the interaction. A similar result was observed using a probe for site STAT1-3 (data not shown). Thus, STAT1-2/3 sites contribute to the up-regulation of PKC $\epsilon$  transcriptional activity in breast cancer cells.

Next, we carried out similar experiments to determine whether the Sp1-2 site was implicated in PKC $\epsilon$  up-regulation in breast cancer cells relative to nontumorigenic MCF-10A cells. As shown in Fig. 6A, deletion of fragment -777 to -531 bp, which includes relevant Sp1-2 site in region A (position -668 to -659), reduced luciferase reporter activity in MCF-7 cells but not in MCF-10A cells. No additional changes were found upon deletion of region -531 to -320 bp in either cell line. To verify the relevance of the Sp1-2 site in PKC $\epsilon$  up-regulation in breast cancer cells, we compared the activity of pGL3-777/+219 (wild type) versus pGL3-777/+219 (Sp1-2-mutated) in MCF-7 and MCF-10A cells. Fig. 7A shows that mutation of Sp1-2 significantly reduced luciferase activity in MCF-7 cells,

whereas this mutation had no effect in MCF-10A cells. As expected, mutation of the Sp1-1 site, which was dispensable for transcriptional activity (see Fig. 4C), did not alter reporter activity in MCF-7 or MCF-10A cells. To further verify the relevance of the Sp1-2 site in PKC $\epsilon$  up-regulation in breast cancer, we used an EMSA approach. Nuclear extracts from MCF-10A, MCF-7, or T-47D cells were incubated with radiolabeled probes for either the Sp1-2 site or a standard Sp1 binding consensus. As shown in Fig. 7B, a shift protein-DNA complex band was detected after incubation of nuclear extracts from either probe both in MCF-7 (lanes 3 and 6) and T-47D cells (lanes 4 and 7) but not in nontumorigenic MCF-10A cells (lanes 2 and 5). The specificity of the interaction was confirmed by competition of the shift band with an excess (50-fold molar) of unlabeled probes for either Sp1-2 (Fig. 7B, lane 8) or a standard Sp1 binding consensus (lane 9) but not with an unlabeled probe for AP-1 (lane 10).

We also found that deletion of fragment -320 to -105 bp, which comprises proximal Sp1-binding sites (Sp1-6/7), essentially abolished luciferase activity both in MCF-7 and MCF-10A

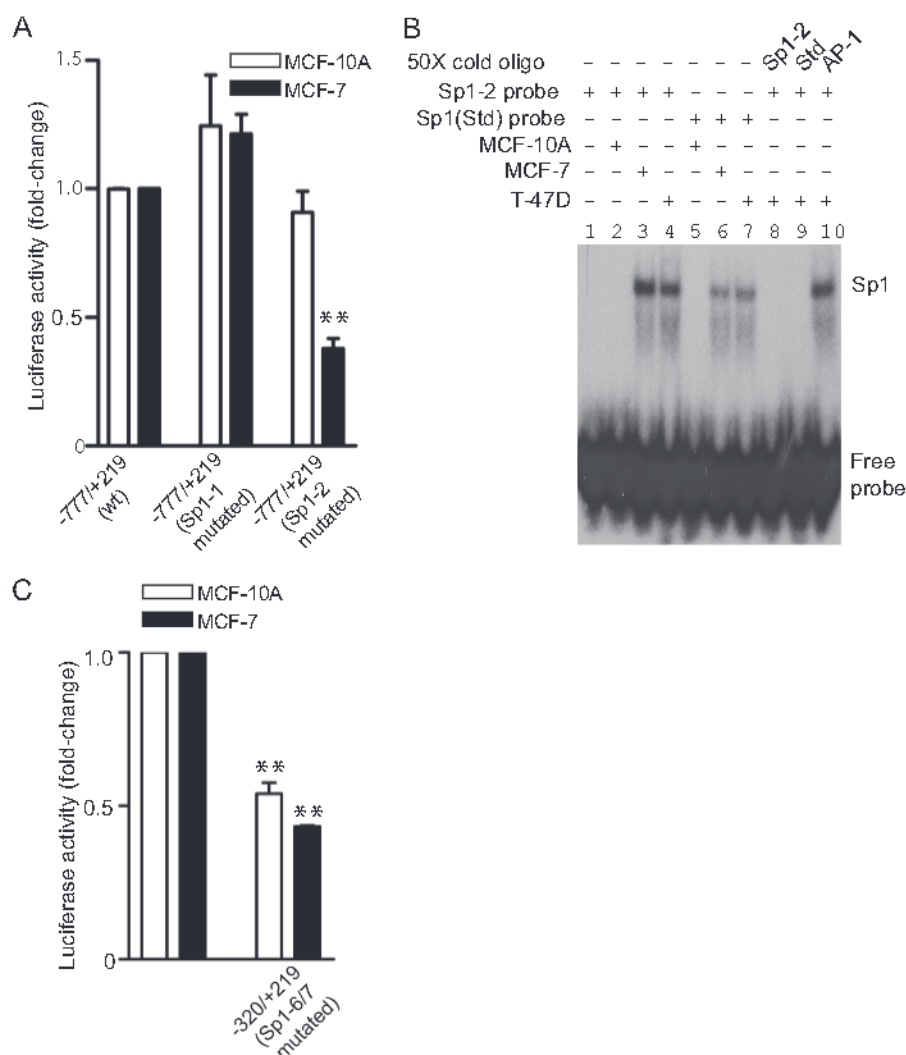


**FIGURE 7. Contribution of Sp1-2 site to PKC $\epsilon$  overexpression in breast cancer cells.** *A*, mutation of Sp1-2 site decreases PKC $\epsilon$  promoter activity in MCF-7 breast cancer cells but not in MCF-10A cells. Luciferase activity of pGL3-777/+219 (wild-type, Sp1-1 site mutant, or Sp1-2 site mutant) was determined 48 h after transfection. Data are expressed as mean  $\pm$  S.E. of three individual experiments. Luciferase activity of wild-type pGL3-777/+219 construct was set as 1. \*\*,  $p < 0.01$  versus pGL3-777/+219 (WT). *B*, elevated Sp1-DNA binding activity in MCF-7 and T-47D breast cancer cells, as determined by EMSA. Similar results were observed in two independent experiments. *C*, mutation of Sp1-6/7 sites reduces PKC $\epsilon$  promoter activity both in MCF-7 and MCF-10A cells. Luciferase activity of pGL3-320/+219 (wild-type or Sp1-6/7 sites mutant) was determined 48 h after transfection. Data are expressed as mean  $\pm$  S.E. of three individual experiments. Luciferase activity of wild-type pGL3-320/+219 construct was set as 1. \*\*,  $p < 0.01$  versus pGL3-320/+219 (wt).

cells (see Fig. 6A). Mutation of Sp1-6/7 sites significantly reduced the activity of the pGL3-320/+219 reporter in MCF-7 and MCF-10A cells (Fig. 7C), suggesting that Sp1-6/7 may control constitutive expression both in normal and cancer cells. The large drop in activity by deletion of fragment -320 to -105 bp compared with the mutation of Sp1-6/7 sites (Fig. 6A see also Fig. 3) argues for additional elements in this region controlling basal promoter activity.

**PKC $\epsilon$  Controls Its Own Expression in Breast Cancer Cells—**There is evidence that PKC $\epsilon$  controls the phosphorylation status and activity of STAT1 in several cellular models (36–38). Ser-727 phosphorylation in STAT1 is required for its maximal transcriptional activity (39). Likewise, we found that PKC $\epsilon$  controls the activation status of STAT1 in breast cancer cells, as judged by the reduction in phospho-Ser-727-STAT1 levels upon PKC $\epsilon$  depletion in MCF-7, T-47D, MDA-MD-231, MDA-MB-453, and MDA-MB-468 breast cancer cell lines (Fig. 8A). Similar results were observed in prostate and lung cancer

models (data not shown). Treatment of MCF-7 cells with the pan-PKC inhibitor GF 109203X or the specific PKC $\epsilon$  inhibitor  $\epsilon$ V1-2 also reduced phospho-Ser727-STAT1 levels (Fig. 8B). Given our finding that STAT1 transcriptionally regulates PKC $\epsilon$  expression, we speculated that PKC $\epsilon$  controls its own expression via STAT1. Treatment of MCF-7 cells with  $\epsilon$ V1-2 (Fig. 8C) or GF 109203X (data not shown) significantly reduced pGL3-1416/+219 luciferase reporter activity. To examine the potential involvement of PKC $\epsilon$  in controlling its own promoter activity, we used PKC $\epsilon$  RNAi. PKC $\epsilon$  expression was silenced from MCF-7 cells by >90% upon delivery of two different PKC $\epsilon$  RNAi duplexes ( $\epsilon$ 1 and  $\epsilon$ 2), as we did previously in other models (18, 25). Notably, luciferase activity of the pGL3-1416/+219 reporter was significantly decreased in PKC $\epsilon$ -depleted MCF-7 cells (Fig. 8D), indicating that the elevated levels of PKC $\epsilon$  in breast cancer cells positively control its own expression at a transcriptional level. The results described above argue for a mutual dependence between PKC $\epsilon$  expres-



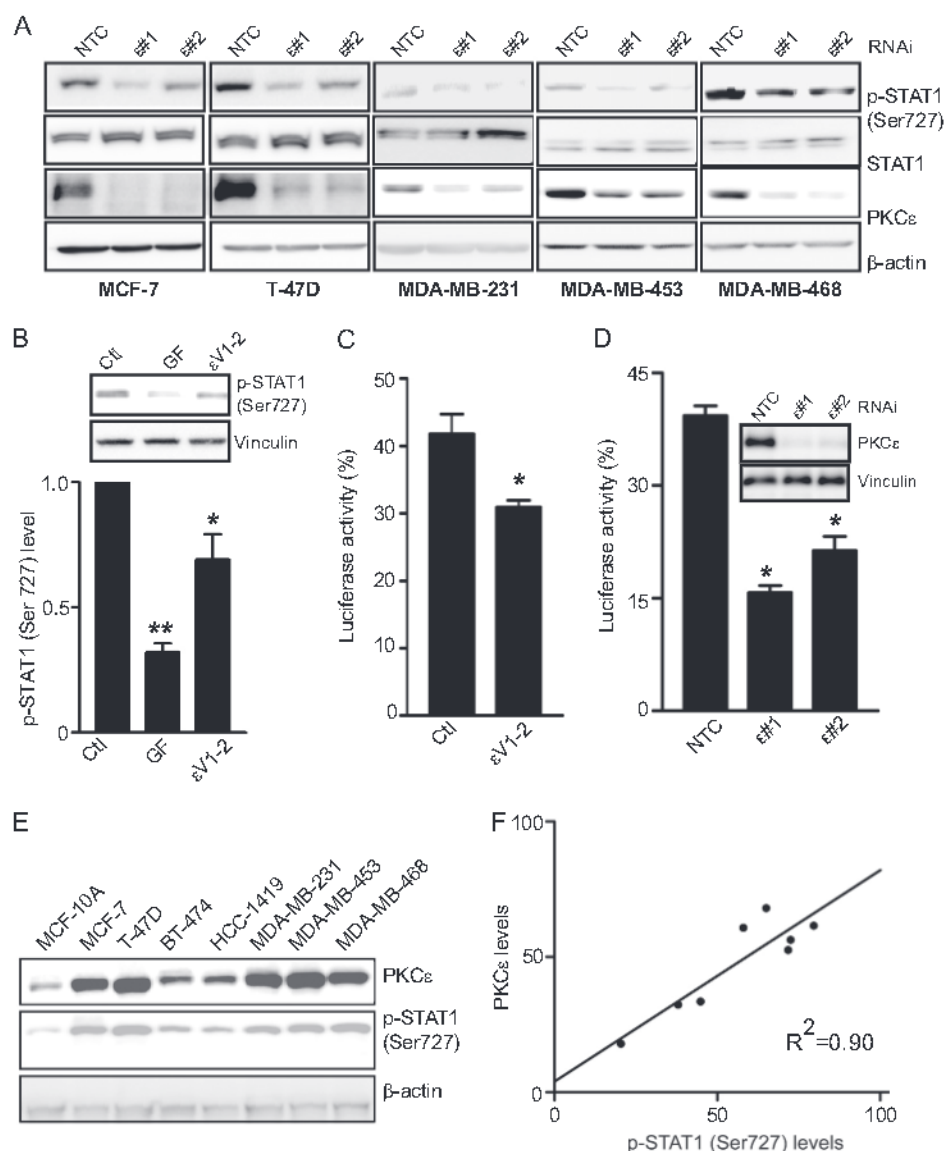


**FIGURE 8. Correlation between PKC $\epsilon$  expression levels and STAT1 activation status.** *A*, PKC $\epsilon$  RNAi depletion reduces phospho-Ser-727-STAT1 levels in breast cancer cell lines. MCF-7, T-47D, MDA-MB-231, MDA-MB-453, and MDA-MB-468 cells were transiently transfected with PKC $\epsilon$  (1 or 2) or nontarget control (NTC) RNAi duplexes. After 72 h, levels of phospho-Ser-727-STAT1 and total STAT1 were determined by Western blot. A second experiment gave similar results. *B*, effect of pan-PKC inhibitor GF109203X (5  $\mu$ M, 24 h) or the PKC $\epsilon$  inhibitor  $\epsilon$ V1-2 (1  $\mu$ M, 24 h) on phospho-Ser-727-STAT1 levels in MCF-7 cells, as determined by Western blot (upper panel). A representative experiment is shown, together with densitometric analysis. Data are expressed as mean  $\pm$  S.E. of four individual experiments. \*,  $p < 0.05$ ; \*\*,  $p < 0.01$  versus control. *C*, inhibition of pGL3-1416/+219 reporter activity in MCF-7 cells by  $\epsilon$ V1-2 (1  $\mu$ M, 24 h). Luciferase activity of construct pGL3-1416/+219 was determined 48 h after transfection. Data are expressed as mean  $\pm$  S.D. of triplicate samples. Two additional experiments gave same results. \*,  $p < 0.05$  versus control. *D*, inhibition of pGL3-1416/+219 reporter activity by PKC $\epsilon$  RNAi. MCF-7 cells were transiently transfected with PKC $\epsilon$  (1 or 2) or nontarget control RNAi duplexes. After 24 h, pGL3-1416/+219 was transiently transfected into MCF-7 cells along with the pRL-TK *Renilla* luciferase vector. Luciferase activity was determined 48 h later. Data are expressed as mean  $\pm$  S.D. of triplicate samples. Two additional experiments gave same results. \*,  $p < 0.05$  versus control. *Inset*, PKC $\epsilon$  expression, as determined by Western blot. *E*, PKC $\epsilon$  and phospho-Ser-727-STAT1 levels in mammary cell lines, as determined by Western blot. Similar results were observed in three independent experiments. *F*, correlation between expression levels of PKC $\epsilon$  and phospho-Ser-727-STAT1 levels in mammary cell lines.

sion and STAT1 activation. We decided to formally test this hypothesis in mammary cellular models (Fig. 8E). We observed that normal immortalized MCF-10A cells, which express low PKC $\epsilon$  levels, display low levels of phospho-Ser-727-STAT1. Conversely, breast cancer cell lines with very high PKC $\epsilon$  levels (MCF-7, T-47D, MDA-MB-231, MDA-MB-453, and MDA-MB-468) show high levels of phospho-Ser-727-STAT1. Breast cancer cell lines with intermediate PKC $\epsilon$  levels (BT-474 and HCC-1419) show intermediate phospho-Ser-727-STAT1 signals by Western blot. Upon densitometric quantification of

Western blots, we found a strong correlation between PKC $\epsilon$  and phospho-Ser-727-STAT1 levels ( $R^2 = 0.90$ ) (Fig. 8F). Altogether, these results argue for a positive feedback between PKC $\epsilon$  expression and STAT1 activation in breast cancer cells.

**PKC $\epsilon$  Mediates Migration of Breast Cancer Cells**—PKC $\epsilon$  has been implicated in tumor initiation, progression, and metastasis (22, 25, 27). Fig. 9A shows that PKC $\epsilon$  RNAi depletion significantly reduced the motility of cells in response to 5% FBS, as determined with a Boyden chamber. The Sp1 inhibitor MTM, which significantly reduces PKC $\epsilon$  expression (Fig. 9B, see also

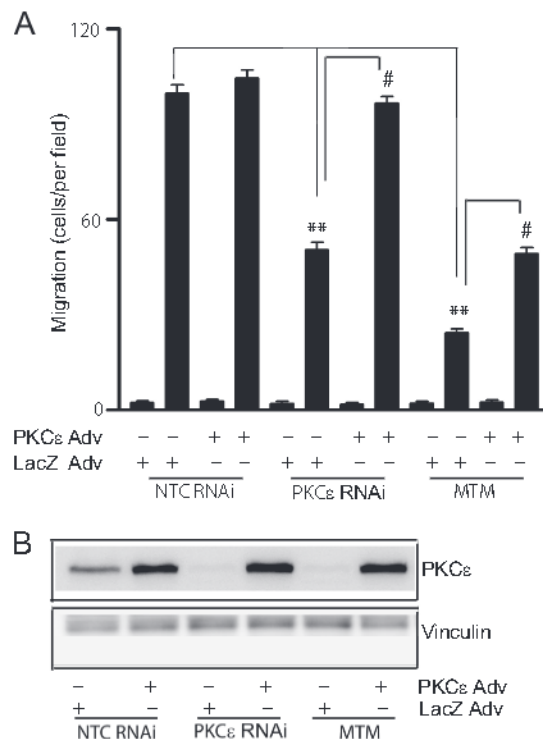


**FIGURE 9. PKC $\epsilon$  RNAi depletion and Sp1 inhibition impair breast cancer cell migration.** MCF-7 cells were transfected with PKC $\epsilon$  or nontarget control (NTC) RNAi duplexes. After 24 h, MCF-7 cells were infected with either control LacZ adenovirus or PKC $\epsilon$  adenovirus (multiplicity of infection = 0.5 pfu/cell) or were treated with the Sp1 inhibitor MTM (30 nM). After 48 h, migration in response to 5% FBS was determined using a Boyden chamber. A, migrated cells were counted from five independent fields. Data are expressed as mean  $\pm$  S.D. ( $n = 3$ ). \*\*,  $p < 0.01$ ; #,  $p < 0.01$ . B, expression of PKC $\epsilon$ , as determined by Western blot. Similar results were obtained in two independent experiments.

Figs. 4F and 5F) also significantly impaired MCF-7 cell migration (Fig. 9A). Adenoviral overexpression of PKC $\epsilon$  overcame the effect of PKC $\epsilon$  RNAi on cell migration. The impaired cell migration caused by MTM could be partially restored by adenoviral overexpression of PKC $\epsilon$ , thus arguing that the expression levels of PKC $\epsilon$  are crucial for the ability of breast cancer cells to migrate.

## DISCUSSION

PKC $\epsilon$ , a member of the novel PKCs, has been extensively characterized as a mitogenic/survival kinase that activates pathways linked to malignant transformation and metastasis, including Ras/Raf/Erk, PI3K/Akt, and NF- $\kappa$ B (17, 18). Pharmacological inhibition or RNAi silencing of PKC $\epsilon$  expression impairs the ability of cancer cells to form tumors in nude mice and metastasize to distant sites (22). Overexpression of PKC $\epsilon$  in nontransformed cells confers growth/survival advantage or leads to malignant transformation (16). In an *in vivo* scenario, transgenic overexpression of PKC $\epsilon$  in the mouse prostate leads to a preneoplastic phenotype, and skin transgenic overexpression of this kinase leads to the development of metastatic squamous carcinoma (40). Therefore, there is significant evidence that overexpression of PKC $\epsilon$  is causally associated with the development of a malignant and metastatic phenotype. This is highly relevant in the context of human cancer, as a vast majority of cancers displays PKC $\epsilon$  up-regulation, including breast,

prostate, and lung cancer (18, 22, 25). Increased PKC $\epsilon$  expression in breast cancer correlates with high histological grade, positive ErbB2/Her2 status, and hormone-independent status (22). Despite the wealth of functional information regarding PKC and cancer, both *in vitro* and *in vivo*, as well as the established mechanistic links with proliferative pathways, the causes behind the up-regulation of PKC $\epsilon$  in human cancer remained elusive.

In this study we report that PKC $\epsilon$  up-regulation in breast cancer cells occurs through dysregulation of transcriptional mechanisms. An  $\sim 1.6$ -kb fragment of human genomic DNA encompassing the 5'-flanking region and part of the first exon ( $-1.4$  to  $+0.2$  kb) of the *PRKCE* gene was isolated and cloned into a luciferase reporter vector. This fragment displayed significantly higher transcriptional activity when expressed in breast cancer cells relative to normal immortalized MCF-10A cells. However, the elevated PKC $\epsilon$  mRNA levels in breast cancer cells do not seem to be related to changes in mRNA stability. Our deletional and mutagenesis studies combined with *in silico* analysis identified key positive regulatory *cis*-acting Sp1 and STAT1 elements in two regions (regions A and B) that we defined as responsible for the up-regulation of PKC $\epsilon$  transcriptional activation in breast cancer cells, and their functional relevance was confirmed by EMSA and ChIP. A region that negatively regulates transcription located upstream from the 1.6-kb fragment, specifically between  $-1.4$  and  $-1.9$  kb, was also identified. Studies to dissect and characterize these negative elements are underway.

From the seven putative Sp1-responsive elements located in region A of the *PRKCE* gene, only one located between bp  $-668$  and  $-659$  contributes to the differential overexpression of PKC $\epsilon$  in MCF-7 cells. The two most proximal Sp1 sites located in positions  $-269/-260$  and  $-256/-247$  contribute to transcriptional activation of the *PRKCE* gene both in MCF-7 and MCF-10A cells, suggesting that these sites control basal expression both in normal and cancer cells. The Sp1 transcription factor has been widely implicated in cancer and is up-regulated in human tumors. For example, it has been reported that Sp1 protein and binding activity are elevated in human breast carcinoma (41, 42). Sp1 is highly expressed both in estrogen receptor-positive and -negative cell lines (43), and its depletion using RNAi leads to reduced G<sub>1</sub>/S progression of breast cancer cells (44). Sp1 controls the expression of genes implicated in breast tumorigenesis and metastatic dissemination, including ErbB2 (45), EGF receptor (46), IGF-IR (47, 48), VEGF (49, 50), cyclin D1 (51), and urokinase-type plasminogen activator receptor (42). The transcription factor Sp1 binds to GC-rich motifs in DNA, and DNA methylation of CpG islands can inhibit Sp1 binding to DNA (52–54). Nevertheless, our studies show that the demethylating agent AZA could not up-regulate PKC $\epsilon$  mRNA levels in MCF-10A cells. Thus, despite the presence of CpG-rich regions in the *PRKCE* promoter, repression by methylation does not seem to take place in normal mammary cells. It is interesting that a recent study in ventricular myocytes showed *PRKCE* gene repression through methylation of Sp1 sites via reactive oxygen species in response to norepinephrine or hypoxia (55, 56), suggesting that epigenetic regulation of the *PRKCE* gene can take place in some cell types under specific

conditions. Notably, functional Sp1-binding sites have been identified in the promoters of PKC $\beta$  and PKC $\delta$  isozymes, and Sp1 binding to the PKC $\beta$  gene is repressed by hypermethylation and re-expressed by AZA treatment (57, 58).

The most notable characteristic of region B in the *PRKCE* promoter is the presence of three STAT1-binding sites. Two of those sites located in position  $-880/-869$  and  $-793/-782$  are functionally relevant in breast cancer cells. Indeed, a marked reduction ( $>50\%$ ) of promoter activity was observed upon mutation of these sites. Moreover, STAT1 RNAi caused a significant reduction in PKC $\epsilon$  mRNA and protein levels. The elevated PKC $\epsilon$  levels in breast cancer cell lines strongly correlate with the activation status of STAT1. Activation of STAT transcription factors involves the phosphorylation of tyrosine residues either by JAK or independently of JAK by tyrosine kinase receptors such as EGF receptor (59). To date, the role of STAT1 in cancer progression remains controversial. Based on its canonical role in IFN- $\gamma$  signaling and loss of function studies using STAT1 knock-out mice, it has been postulated that STAT1 acts as a tumor suppressor (60). However, a large number of studies link STAT1 with tumor promotion as well as with resistance to chemotherapy and radiotherapy. Moreover, STAT1 is up-regulated and/or hyperactive in many cancers, including breast cancer (61, 62). STAT1 up-regulation in human breast cancer is associated with metastatic dissemination and poor outcome in patients (62–64). In addition, STAT1 overexpression has been linked to aggressive tumor growth and the induction of proinflammatory factors, whereas STAT1 knockdown delays tumor progression (61). Inhibition of STAT1 in breast cancer prevents the homing of suppressive immune cells to the tumor microenvironment and enables immune-mediated tumor rejection (61). ErbB receptor activation, a common event in human breast cancer, significantly enhances STAT1 expression (65). In other models, such as melanoma, suppression of STAT1 expression reduces cell motility, invasion, and metastatic dissemination (66). STAT1 expression correlates with resistance to chemotherapeutic agents such as doxorubicin, docetaxel, and platinum compounds and is elevated in resistant tumors (67–72). STAT1 also promotes radioresistance of breast cancer stem cells (73). Notably, PKC $\epsilon$  has been linked to chemo- and radio-resistance (19, 20); thus, it is conceivable that PKC $\epsilon$  up-regulation mediated by STAT1 may play a role in this context. The fact that PKC $\epsilon$  controls its own expression in breast cancer cells suggests the possibility of a vicious cycle that contributes to the overexpression of this kinase. It is unclear at this stage what pathways are controlled by PKC $\epsilon$  that lead to its own transcriptional activation. One possibility is that PKC $\epsilon$  controls the expression of factors that influence STAT1 activation status, such as growth factors or cytokines that signal via this transcription factor.

In summary, this study identified relevant mechanisms that control PKC $\epsilon$  expression in breast cancer cells. As PKC $\epsilon$  overexpression has been linked to an aggressive phenotype and metastatic dissemination, our study may have significant therapeutic implications. In this regard, several studies suggested that targeting PKC $\epsilon$  could be an effective anticancer strategy. Indeed, the PKC $\epsilon$  translocation inhibitor  $\epsilon$ V1-2 has anti-tumorigenic activity in non-small cell lung cancer and

head and neck squamous cell carcinoma models (25, 27). More recently, an ATP mimetic inhibitor with selectivity for PKC $\epsilon$  was shown to impair the growth of MDA-MB-231 breast cancer xenografts in mice as well as to reverse Ras-driven and epithelial-mesenchymal transition-dependent phenotypes in breast cancer cells (26). Thus, targeting PKC $\epsilon$  or the mechanisms responsible for its up-regulation in tumors may provide novel means for the treatment of cancer types driven by PKC $\epsilon$  overexpression.

## REFERENCES

- Kampfer, S., Windeger, M., Hochholdinger, F., Schwaiger, W., Pestell, R. G., Baier, G., Grunicke, H. H., and Uberall, F. (2001) Protein kinase C isoforms involved in the transcriptional activation of cyclin D1 by transforming Ha-Ras. *J. Biol. Chem.* **276**, 42834–42842
- Mesquita, R. F., Paul, M. A., Valmaseda, A., Francois, A., Jabr, R., Anjum, S., Marber, M. S., Budhram-Mahadeo, V., and Heads, R. J. (2014) Protein kinase C $\epsilon$ -calcineurin cosignaling downstream of toll-like receptor 4 downregulates fibrosis and induces wound healing gene expression in cardiac myofibroblasts. *Mol. Cell Biol.* **34**, 574–594
- Quann, E. J., Liu, X., Altan-Bonnet, G., and Huse, M. (2011) A cascade of protein kinase C isoforms promotes cytoskeletal polarization in T cells. *Nat. Immunol.* **12**, 647–654
- Saurin, A. T., Durgan, J., Cameron, A. J., Faisal, A., Marber, M. S., and Parker, P. J. (2008) The regulated assembly of a PKC $\epsilon$  complex controls the completion of cytokinesis. *Nat. Cell Biol.* **10**, 891–901
- Soh, J. W., and Weinstein, I. B. (2003) Roles of specific isoforms of protein kinase C in the transcriptional control of cyclin D1 and related genes. *J. Biol. Chem.* **278**, 34709–34716
- Wu, D. F., Chandra, D., McMahon, T., Wang, D., Dadgar, J., Kharaznia, V. N., Liang, Y. J., Waxman, S. G., Dib-Hajj, S. D., and Messing, R. O. (2012) PKC $\epsilon$  phosphorylation of the sodium channel NaV1.8 increases channel function and produces mechanical hyperalgesia in mice. *J. Clin. Invest.* **122**, 1306–1315
- Churchill, E. N., Ferreira, J. C., Brum, P. C., Szweda, L. L., and Mochly-Rosen, D. (2010) Ischaemic preconditioning improves proteasomal activity and increases the degradation of  $\delta$ PKC during reperfusion. *Cardiovasc. Res.* **85**, 385–394
- Jornayvaz, F. R., and Shulman, G. I. (2012) Diacylglycerol activation of protein kinase C $\epsilon$  and hepatic insulin resistance. *Cell Metab.* **15**, 574–584
- Lee, A. M., and Messing, R. O. (2011) Protein kinase C $\epsilon$  modulates nicotine consumption and dopamine reward signals in the nucleus accumbens. *Proc. Natl. Acad. Sci. U.S.A.* **108**, 16080–16085
- Zhang, D., Christianson, J., Liu, Z. X., Tian, L., Choi, C. S., Neschen, S., Dong, J., Wood, P. A., and Shulman, G. I. (2010) Resistance to high-fat diet-induced obesity and insulin resistance in mice with very long-chain acyl-CoA dehydrogenase deficiency. *Cell Metab.* **11**, 402–411
- Cacace, A. M., Guadagno, S. N., Krauss, R. S., Fabbro, D., and Weinstein, I. B. (1993) The  $\epsilon$  isoform of protein kinase C is an oncogene when overexpressed in rat fibroblasts. *Oncogene* **8**, 2095–2104
- Su, T., Straight, S., Bao, L., Xie, X., Lehner, C. L., Cavey, G. S., Teknos, T. N., and Pan, Q. (2013) PKC $\epsilon$  phosphorylates and mediates the cell membrane localization of RhoA. *ISRN Oncol.* **2013**, 329063
- Griner, E. M., and Kazanietz, M. G. (2007) Protein kinase C and other diacylglycerol effectors in cancer. *Nat. Rev. Cancer* **7**, 281–294
- Garg, R., Benedetti, L. G., Abera, M. B., Wang, H., Abba, M., and Kazanietz, M. G. (2013) Protein kinase C and cancer: what we know and what we do not. *Oncogene* **10.1038/onc.2013.524**
- Mischak, H., Goodnight, J. A., Kolch, W., Martiny-Baron, G., Schaeuble, C., Kazanietz, M. G., Blumberg, P. M., Pierce, J. H., and Mushinski, J. F. (1993) Overexpression of protein kinase C- $\delta$  and  $\epsilon$  in NIH 3T3 cells induces opposite effects on growth, morphology, anchorage dependence, and tumorigenicity. *J. Biol. Chem.* **268**, 6090–6096
- Perletti, G. P., Folini, M., Lin, H. C., Mischak, H., Piccinini, F., and Tashjian, A. H., Jr. (1996) Overexpression of protein kinase C $\epsilon$  is oncogenic in rat colonic epithelial cells. *Oncogene* **12**, 847–854



17. Benavides, F., Blando, J., Perez, C. J., Garg, R., Conti, C. J., DiGiovanni, J., and Kazanietz, M. G. (2011) Transgenic overexpression of PKC $\epsilon$  in the mouse prostate induces preneoplastic lesions. *Cell Cycle* **10**, 268–277
18. Garg, R., Blando, J., Perez, C. J., Wang, H., Benavides, F. J., and Kazanietz, M. G. (2012) Activation of nuclear factor  $\kappa$ B (NF- $\kappa$ B) in prostate cancer is mediated by protein kinase C $\epsilon$  (PKC $\epsilon$ ). *J. Biol. Chem.* **287**, 37570–37582
19. Ding, L., Wang, H., Lang, W., and Xiao, L. (2002) Protein kinase C- $\epsilon$  promotes survival of lung cancer cells by suppressing apoptosis through dysregulation of the mitochondrial caspase pathway. *J. Biol. Chem.* **277**, 35305–35313
20. Körner, C., Keklikoglou, L., Bender, C., Wörner, A., Münstermann, E., and Wiemann, S. (2013) MicroRNA-31 sensitizes human breast cells to apoptosis by direct targeting of protein kinase C $\epsilon$  (PKC $\epsilon$ ). *J. Biol. Chem.* **288**, 8750–8761
21. Shankar, E., Sivaprasad, U., and Basu, A. (2008) Protein kinase C $\epsilon$  confers resistance of MCF-7 cells to TRAIL by Akt-dependent activation of Hdm2 and downregulation of p53. *Oncogene* **27**, 3957–3966
22. Pan, Q., Bao, L. W., Kleer, C. G., Sabel, M. S., Griffith, K. A., Teknos, T. N., and Merajver, S. D. (2005) Protein kinase C $\epsilon$  is a predictive biomarker of aggressive breast cancer and a validated target for RNA interference anti-cancer therapy. *Cancer Res.* **65**, 8366–8371
23. Wu, D., Foreman, T. L., Gregory, C. W., McJilton, M. A., Wescott, G. G., Ford, O. H., Alvey, R. F., Mohler, J. L., and Terrian, D. M. (2002) Protein kinase C $\epsilon$  has the potential to advance the recurrence of human prostate cancer. *Cancer Res.* **62**, 2423–2429
24. Aziz, M. H., Manoharan, H. T., Church, D. R., Dreckschmidt, N. E., Zhong, W., Oberley, T. D., Wilding, G., and Verma, A. K. (2007) Protein kinase C $\epsilon$  interacts with signal transducers and activators of transcription 3 (Stat3), phosphorylates Stat3Ser727, and regulates its constitutive activation in prostate cancer. *Cancer Res.* **67**, 8828–8838
25. Caino, M. C., Lopez-Haber, C., Kissil, J. L., and Kazanietz, M. G. (2012) Non-small cell lung carcinoma cell motility, rac activation and metastatic dissemination are mediated by protein kinase C $\epsilon$ . *PLoS One* **7**, e31714
26. Dann, S. G., Golas, J., Miranda, M., Shi, C., Wu, J., Jin, G., Rosford, E., Upeklis, E., and Klippel, A. (2013) p120 catenin is a key effector of a Ras-PKC $\epsilon$  oncogenic signaling axis. *Oncogene*
27. Caino, M. C., Lopez-Haber, C., Kim, J., Mochly-Rosen, D., and Kazanietz, M. G. (2012) Protein kinase C $\epsilon$  is required for non-small cell lung carcinoma growth and regulates the expression of apoptotic genes. *Oncogene* **31**, 2593–2600
28. Wang, H., Xiao, L., and Kazanietz, M. G. (2011) p23/Tmp21 associates with protein kinase C $\delta$  (PKC $\delta$ ) and modulates its apoptotic function. *J. Biol. Chem.* **286**, 15821–15831
29. Taminiau, J., Meganck, S., Lazar, C., Steenhoff, D., Coletta, A., Molter, C., Duque, R., de Schaetzen, V., Weiss Solis, D. Y., Bersini, H., and Nowé, A. (2012) Unlocking the potential of publicly available microarray data using inSilicoDb and inSilicoMerging R/Bioconductor packages. *BMC Bioinformatics* **13**, 335
30. Gutiérrez-Uzquiza, A., Árecherra, M., Bragado, P., Aguirre-Ghiso, J. A., and Porras, A. (2012) p38 $\alpha$  mediates cell survival in response to oxidative stress via induction of antioxidant genes: effect on the p70S6K pathway. *J. Biol. Chem.* **287**, 2632–2642
31. Lopez-Haber, C., and Kazanietz, M. G. (2013) Cucurbitacin I inhibits Rac1 activation in breast cancer cells by a reactive oxygen species-mediated mechanism and independently of Janus tyrosine kinase 2 and P-Rex1. *Mol. Pharmacol.* **83**, 1141–1154
32. Bae, K. M., Wang, H., Jiang, G., Chen, M. G., Lu, L., and Xiao, L. (2007) Protein kinase C $\epsilon$  is overexpressed in primary human non-small cell lung cancers and functionally required for proliferation of non-small cell lung cancer cells in a p21/Cip1-dependent manner. *Cancer Res.* **67**, 6053–6063
33. Martínez-Gimeno, C., Díaz-Meco, M. T., Domínguez, I., and Moscat, J. (1995) Alterations in levels of different protein kinase C isoforms and their influence on behavior of squamous cell carcinoma of the oral cavity: pPKC, a novel prognostic factor for relapse and survival. *Head Neck* **17**, 516–525
34. Albertini, V., Jain, A., Vignati, S., Napoli, S., Rinaldi, A., Kwee, L., Nur-e-Alam, M., Bergant, J., Bertoni, F., Carbone, G. M., Rohr, J., and Catapano, C. V. (2006) Novel GC-rich DNA-binding compound produced by a genetically engineered mutant of the mithramycin producer *Streptomyces argillaceus* exhibits improved transcriptional repressor activity: implications for cancer therapy. *Nucleic Acids Res.* **34**, 1721–1734
35. Sastry, M., and Patel, D. J. (1993) Solution structure of the mithramycin dimer-DNA complex. *Biochemistry* **32**, 6588–6604
36. Cheng, M. B., Zhang, Y., Zhong, X., Sutter, B., Cao, C. Y., Chen, X. S., Cheng, X. K., Xiao, L., and Shen, Y. F. (2010) Stat1 mediates an auto-regulation of hsp90 $\beta$  gene in heat shock response. *Cell Signal* **22**, 1206–1213
37. Ivaska, J., Bosca, L., and Parker, P. J. (2003) PKC $\epsilon$  is a permissive link in integrin-dependent IFN- $\gamma$  signalling that facilitates JAK phosphorylation of STAT1. *Nat. Cell Biol.* **5**, 363–369
38. Xuan, Y. T., Guo, Y., Zhu, Y., Wang, O. L., Rokosh, G., Messing, R. O., and Bolli, R. (2005) Role of the protein kinase C- $\epsilon$ -Raf-1-MEK-1/2-p44/42 MAPK signaling cascade in the activation of signal transducers and activators of transcription 1 and 3 and induction of cyclooxygenase-2 after ischemic preconditioning. *Circulation* **112**, 1971–1978
39. Ramana, C. V., Chatterjee-Kishore, M., Nguyen, H., and Stark, G. R. (2000) Complex roles of Stat1 in regulating gene expression. *Oncogene* **19**, 2619–2627
40. Verma, A. K., Wheeler, D. L., Aziz, M. H., and Manoharan, H. (2006) Protein kinase C $\epsilon$  and development of squamous cell carcinoma, the non-melanoma human skin cancer. *Mol. Carcinog.* **45**, 381–388
41. Wang, X. B., Peng, W. Q., Yi, Z. J., Zhu, S. L., and Gan, Q. H. (2007) Expression and prognostic value of transcriptional factor Sp1 in breast cancer. *Ai Zheng* **26**, 996–1000
42. Zannetti, A., Del Vecchio, S., Carriero, M. V., Fonti, R., Franco, P., Botti, G., D'Aiuto, G., Stoppelli, M. P., and Salvatore, M. (2000) Coordinate up-regulation of Sp1 DNA-binding activity and urokinase receptor expression in breast carcinoma. *Cancer Res.* **60**, 1546–1551
43. Mertens-Talcott, S. U., Chinthalapalli, S., Li, X., and Safe, S. (2007) The oncogenic microRNA-27a targets genes that regulate specificity protein transcription factors and the G2-M checkpoint in MDA-MB-231 breast cancer cells. *Cancer Res.* **67**, 11001–11011
44. Abdelrahim, M., Samudio, I., Smith, R., 3rd, Burghardt, R., and Safe, S. (2002) Small inhibitory RNA duplexes for Sp1 mRNA block basal and estrogen-induced gene expression and cell cycle progression in MCF-7 breast cancer cells. *J. Biol. Chem.* **277**, 28815–28822
45. Chen, Y., and Gill, G. N. (1994) Positive and negative regulatory elements in the human erbB-2 gene promoter. *Oncogene* **9**, 2269–2276
46. Salvatori, L., Ravenna, L., Caporusso, F., Principessa, L., Coroniti, G., Frati, L., Russo, M. A., and Petrangeli, E. (2011) Action of retinoic acid receptor on EGFR gene transactivation and breast cancer cell proliferation: Interplay with the estrogen receptor. *Biomed. Pharmacother.* **65**, 307–312
47. Glat, C., Tencer, L., Ravid, D., Sarfstein, R., Liscovitch, M., and Werner, H. (2006) Caveolin-1 up-regulates IGF-I receptor gene transcription in breast cancer cells via Sp1- and p53-dependent pathways. *Exp. Cell Res.* **312**, 3899–3908
48. Maor, S., Mayer, D., Yarden, R. I., Lee, A. V., Sarfstein, R., Werner, H., and Papa, M. Z. (2006) Estrogen receptor regulates insulin-like growth factor-I receptor gene expression in breast tumor cells: involvement of transcription factor Sp1. *J. Endocrinol.* **191**, 605–612
49. Finkenzeller, G., Weindel, K., Zimmermann, W., Westin, G., and Marmé, D. (2004) Activated Neu/ErbB-2 induces expression of the vascular endothelial growth factor gene by functional activation of the transcription factor Sp 1. *Angiogenesis* **7**, 59–68
50. Loureiro, R. M., and D'Amore, P. A. (2005) Transcriptional regulation of vascular endothelial growth factor in cancer. *Cytokine Growth Factor Rev.* **16**, 77–89
51. Lee, R. J., Albanese, C., Fu, M., D'Amico, M., Lin, B., Watanabe, G., Haines, G. K., 3rd, Siegel, P. M., Hung, M. C., Yarden, Y., Horowitz, J. M., Muller, W. J., and Pestell, R. G. (2000) Cyclin D1 is required for transcription by activated Neu and is induced through an E2F-dependent signaling pathway. *Mol. Cell Biol.* **20**, 672–683
52. Cao, Y. X., Jean, J. C., and Williams, M. C. (2000) Cytosine methylation of an Sp1 site contributes to organ-specific and cell-specific regulation of expression of the lung epithelial gene t1 $\alpha$ . *Biochem. J.* **350** Pt 3, 883–890
53. Dong, L., Jin, L., Tseng, H. Y., Wang, C. Y., Wilmott, J. S., Yosufi, B., Yan,

- X. G., Jiang, C. C., Scolyer, R. A., Zhang, X. D., and Guo, S. T. (2013) Oncogenic suppression of PHLPP1 in human melanoma. *Oncogene* 10.1038/onc.2013.420
54. Kitazawa, S., Kitazawa, R., and Maeda, S. (1999) Transcriptional regulation of rat cyclin D1 gene by CpG methylation status in promoter region. *J. Biol. Chem.* **274**, 28787–28793
55. Patterson, A. J., Xiao, D., Xiong, F., Dixon, B., and Zhang, L. (2012) Hypoxia-derived oxidative stress mediates epigenetic repression of PKC $\epsilon$  gene in foetal rat hearts. *Cardiovasc. Res.* **93**, 302–310
56. Xiong, F., Xiao, D., and Zhang, L. (2012) Norepinephrine causes epigenetic repression of PKC $\epsilon$  gene in rodent hearts by activating Nox1-dependent reactive oxygen species production. *FASEB J.* **26**, 2753–2763
57. Hagiwara, K., Ito, H., Murate, T., Miyata, Y., Ohashi, H., and Nagai, H. (2012) PROX1 overexpression inhibits protein kinase C $\beta$ 1 transcription through promoter DNA methylation. *Genes Chromosomes Cancer* **51**, 1024–1036
58. Jin, H., Kanthasamy, A., Anantharam, V., Rana, A., and Kanthasamy, A. G. (2011) Transcriptional regulation of pro-apoptotic protein kinase C $\delta$ : implications for oxidative stress-induced neuronal cell death. *J. Biol. Chem.* **286**, 19840–19859
59. Andl, C. D., Mizushima, T., Oyama, K., Bowser, M., Nakagawa, H., and Rustgi, A. K. (2004) EGFR-induced cell migration is mediated predominantly by the JAK-STAT pathway in primary esophageal keratinocytes. *Am. J. Physiol. Gastrointest. Liver Physiol.* **287**, G1227–G1237
60. Chan, S. R., Vermi, W., Luo, J., Lucini, L., Rickert, C., Fowler, A. M., Lonardi, S., Arthur, C., Young, L. J., Levy, D. E., Welch, M. J., Cardiff, R. D., and Schreiber, R. D. (2012) STAT1-deficient mice spontaneously develop estrogen receptor  $\alpha$ -positive luminal mammary carcinomas. *Breast Cancer Res.* **14**, R16
61. Hix, L. M., Karavitis, J., Khan, M. W., Shi, Y. H., Khazaie, K., and Zhang, M. (2013) Tumor STAT1 transcription factor activity enhances breast tumor growth and immune suppression mediated by myeloid-derived suppressor cells. *J. Biol. Chem.* **288**, 11676–11688
62. Magkou, C., Giannopoulou, I., Theohari, I., Fytou, A., Rafailidis, P., Nomikos, A., Papadimitriou, C., and Nakopoulou, L. (2012) Prognostic significance of phosphorylated STAT-1 expression in premenopausal and postmenopausal patients with invasive breast cancer. *Histopathology* **60**, 1125–1132
63. Greenwood, C., Metodieva, G., Al-Janabi, K., Lausen, B., Alldridge, L., Leng, L., Bucala, R., Fernandez, N., and Metodiev, M. V. (2012) Stat1 and CD74 overexpression is co-dependent and linked to increased invasion and lymph node metastasis in triple-negative breast cancer. *J. Proteomics* **75**, 3031–3040
64. Rajski, M., Vogel, B., Baty, F., Rochlitz, C., and Buess, M. (2012) Global gene expression analysis of the interaction between cancer cells and osteoblasts to predict bone metastasis in breast cancer. *PLoS One* **7**, e29743
65. Han, W., Carpenter, R. L., Cao, X., and Lo, H. W. (2013) STAT1 gene expression is enhanced by nuclear EGFR and HER2 via cooperation with STAT3. *Mol. Carcinog.* **52**, 959–969
66. Schultz, J., Koczan, D., Schmitz, U., Ibrahim, S. M., Pilch, D., Landsberg, J., and Kunz, M. (2010) Tumor-promoting role of signal transducer and activator of transcription (Stat)1 in late-stage melanoma growth. *Clin. Exp. Metastasis* **27**, 133–140
67. Fryknäs, M., Dhar, S., Oberg, F., Rickardson, L., Rydåker, M., Göransson, H., Gustafsson, M., Pettersson, U., Nygren, P., Larsson, R., and Isaksson, A. (2007) STAT1 signaling is associated with acquired crossresistance to doxorubicin and radiation in myeloma cell lines. *Int. J. Cancer* **120**, 189–195
68. Khodarev, N. N., Beckett, M., Labay, E., Darga, T., Roizman, B., and Weichselbaum, R. R. (2004) STAT1 is overexpressed in tumors selected for radioresistance and confers protection from radiation in transduced sensitive cells. *Proc. Natl. Acad. Sci. U.S.A.* **101**, 1714–1719
69. Khodarev, N. N., Roizman, B., and Weichselbaum, R. R. (2012) Molecular pathways: interferon/stat1 pathway: role in the tumor resistance to genotoxic stress and aggressive growth. *Clin. Cancer Res.* **18**, 3015–3021
70. Patterson, S. G., Wei, S., Chen, X., Sallman, D. A., Gilvary, D. L., Zhong, B., Pow-Sang, J., Yeatman, T., and Djeu, J. Y. (2006) Novel role of Stat1 in the development of docetaxel resistance in prostate tumor cells. *Oncogene* **25**, 6113–6122
71. Rickardson, L., Fryknäs, M., Dhar, S., Lövborg, H., Gullbo, J., Rydåker, M., Nygren, P., Gustafsson, M. G., Larsson, R., and Isaksson, A. (2005) Identification of molecular mechanisms for cellular drug resistance by combining drug activity and gene expression profiles. *Br. J. Cancer* **93**, 483–492
72. Rickardson, L., Fryknäs, M., Haglund, C., Lövborg, H., Nygren, P., Gustafsson, M. G., Isaksson, A., and Larsson, R. (2006) Screening of an annotated compound library for drug activity in a resistant myeloma cell line. *Cancer Chemother. Pharmacol.* **58**, 749–758
73. Franci, C., Zhou, J., Jiang, Z., Modrusan, Z., Good, Z., Jackson, E., and Kouros-Mehr, H. (2013) Biomarkers of residual disease, disseminated tumor cells, and metastases in the MMTV-PyMT breast cancer model. *PLoS One* **8**, e58183

## **Transcriptional Regulation of Oncogenic Protein Kinase C? (PKC?) by STAT1 and Sp1 Proteins**

HongBin Wang, Alvaro Gutierrez-Uzquiza, Rachana Garg, Laura Barrio-Real, Mahlet B. Abera, Cynthia Lopez-Haber, Cinthia Rosemblit, Huaisheng Lu, Martin Abba and Marcelo G. Kazanietz

*J. Biol. Chem.* 2014, 289:19823-19838.

doi: 10.1074/jbc.M114.548446 originally published online May 13, 2014

---

Access the most updated version of this article at doi: [10.1074/jbc.M114.548446](https://doi.org/10.1074/jbc.M114.548446)

### Alerts:

- [When this article is cited](#)
- [When a correction for this article is posted](#)

[Click here](#) to choose from all of JBC's e-mail alerts

This article cites 72 references, 29 of which can be accessed free at <http://www.jbc.org/content/289/28/19823.full.html#ref-list-1>